Microfluidics for Inorganic Chemistry

Ali Abou Hassan, Olivier Sandre, Valérie Cabuil

Author manuscript version of Angewandte Chemie International Edition, 2010. **49**(36): 6268-6286

DOI: 10.1002/anie.200904285

Inorganic in microfluidics

Microfluidics in Inorganic Chemistry

Ali Abou-Hassan, Olivier Sandre and Valérie Cabuil**

Keywords:
microfluidics microreactors liquid-liquid extraction nanomaterials advanced materials

Dedicated to Professor René Massart who taught us inorganic chemistry and discovered a simple route to ionic ferrofluids 30 years ago.

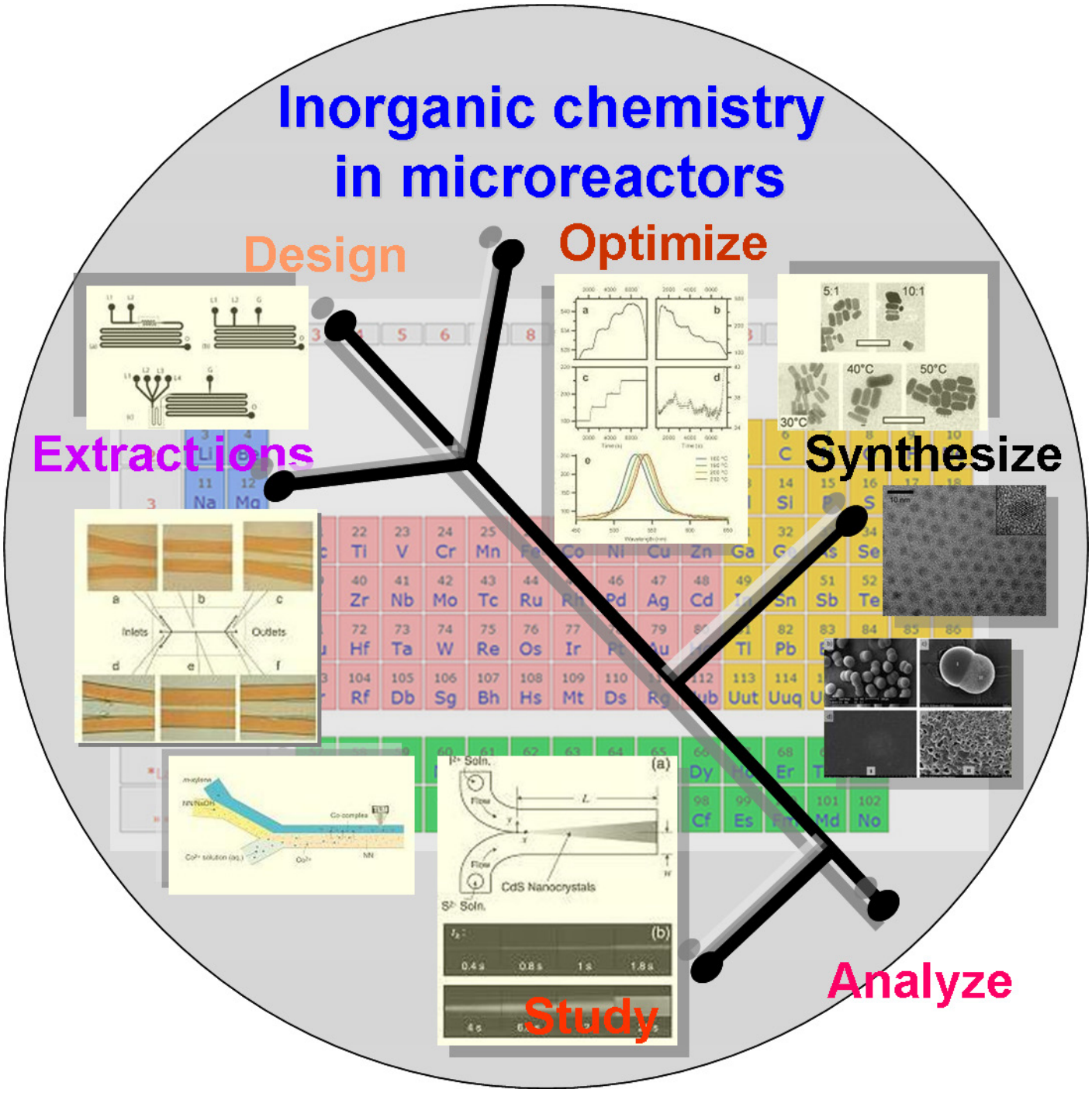

The application of microfluidics in chemistry has gained significant importance in the recent years. Miniaturized chemistry platforms provide controlled fluid transport, rapid chemical reactions and cost-saving advantages over conventional reactors. The advantages of microfluidics have been clearly established in the field of analytical and bioanalytical sciences and in the field of organic synthesis. It is less true in the field of inorganic chemistry and materials science. Yet, inorganic chemistry is mostly concerned by the development of microreactors for the separation and selective extraction of metallic ions. Concerning materials science, microfluidic has been mainly used for the improvement of nanoparticle synthesis, namely metals, metal oxides and semiconductor nanoparticles. Microfluidic devices can also be used for the formulation of more advanced and sophisticated inorganic materials or hybrids.

1. Introduction

Important research efforts in the field of micro scale devices have been devoted to analytical sciences, in order to develop Miniaturised Total Analysis Systems (μ-TAS).[1-4] The idea behind this concept was to combine classical analytical methods and detection elements that could be placed one after the other one to constitute an ideal device that would accomplish all the operations necessary to extract desired informations about particular analytes from a complex mixture: sample preparation, chemical conversions, chemical partitions and signal detection.[1, 5, 6] Besides the continuing development of μ-TAS and related analytical applications, more and more studies tend to establish the benefits provided by microfluidics to the field of chemistry in general.[7, 8] The "lab-on-a-chip" concept emerged to describe a new technology by which each chemical process and system can be miniaturized using microsystem technologies.[9] The key components of a "lab-on-a-chip" devoted to synthesis chemistry are the microreactors. Microreactors have emerged as a particular class of chemical synthesis devices and showed their wide applications for the optimization of reactions and the production of chemicals.[10-15] To date, the outcome of the reported research has confirmed that microreactor methodology is applicable to both gas and liquid phase chemistry.[16, 17] A final dream would be to shrink entire chemistry and analysis laboratories on a single microstructured chip.[18, 19]

The aim of this review is to provide and up-to-date information on microfluidics in the field of inorganic chemistry. The Review is divided into three major sections. In the first one, an overview of available micromixers and microreactors is provided. The following section contains an analysis of the state of the art concerning liquid-liquid extraction of inorganic species using microfluidic devices. Then the synthesis of several classes of nanoparticles and nanomaterials using some of the unique features that microfluidic reactors offer is described. Finally, the last section presents some conclusions and future perspectives of this new technology for inorganic chemistry.

[*] Prof. V. Cabuil[1,2,3]. Dr. O. Sandre[1,2,3] and Dr. A. Abou-Hassan[1,2,3].
1) UPMC Univ Paris 06, UMR 7195 PECSA, Physicochimie des Electrolytes, Colloïdes, Sciences Analytiques, F-75005, Paris France
2) CNRS, UMR 7195 PECSA, Physicochimie des Electrolytes, Colloïdes, Sciences Analytiques, F-75005, Paris France
3) ESPCI, UMR 7195 PECSA, Physicochimie des Electrolytes, Colloïdes, Sciences Analytiques, F-75005, Paris France

E-mail: ali.abou_hassan@upmc.fr; valerie.cabuil@upmc.fr
Homepage : http://www.pecsa.upmc.fr

2. Microfluidics, micromixing and microreactors

Comprehensive and quantitative reviews of fluid behaviour and associated transport processes at the micro-scale have been developed elsewhere.[20, 21] Also, the available microreactors for chemistry have been described in a Review article in Angewandte Chemie,[22] This section aims to briefly point out some basic and important aspects of microfluidics and usual micromixers used in chemistry, that can be useful for the comprehension of the Review.

In general, microfluidics can be defined as the science of systems that process or manipulate minute (10^{-9} to 10^{-18} litres) amounts of fluids, using channels with dimensions of tens to hundreds of micrometers.[11, 23, 24] As systems are reduced in size, phenomena such as diffusion, surface tension and viscosity become ever more important at the micrometer scale.[25] In the case of microfluidic systems with simple geometries, the fluid behaviour is predominantly influenced by viscosity rather than inertia, resulting in laminar flow. Diffusion can be effective for moving and mixing solutes on the micrometer length scales in laminar flow; however mixing only by diffusion in microfluidic systems can be very slow. To overcome this limitation and improve the mixing of fluids, a wide range of microfluidic systems have been designed.[14, 26, 27] These devices are based on the principle that one has to split the liquid stream into a multitude of smaller streams before making them combine. This increases the surface area of interaction between the two fluids that have to be mixed and consequently speeds up the mixing process.[28].

Micromixers are usually categorized as passive micromixers or active micromixers. Passive micromixers do not require external energy; the mixing process relies entirely on diffusion or chaotic advection, whereas active mixers rely on time-dependent perturbations of the fluid flow to achieve mixing.[14, 29-35] Figure 1 shows the laminar and the droplets based micromixers that will be often encountered in this Review as microreactors, for the liquid-liquid extraction or for nanoparticle synthesis. The interested reader

can refer to the reviews of Nguyen et al.[26] and Hessel et al.[36] for a detailed account on micromixing.

Because of their small dimensions, micromixers offer several advantages for the chemical processing.[37] Process parameters such as pressure, temperature, residence time and flow rate can be easily controlled.[10] The hydrodynamic flow in the microchannels is essentially laminar, directed and highly symmetric compared to macroscale conduits in which flow regimes are always turbulent.[38] Mixing times in micromixers are smaller than in conventional systems and, due to the small dimensions, the diffusion times are very short, enabling to control and create rapidly a homogeneous reactant mixture.[14, 39]. Moreover, due to their important surface-to-volume ratio, microfluidic reactors can afford a high heat – exchanging efficiency compared to the one of traditional heat exchangers, allowing to heat or cool the reaction mixture within the microstructure rapidly and work under isothermal conditions with exactly defined residence times.[10, 37, 40] The small reactor volumes (nL - µL) result in minimal reagent consumption and fast responses to system perturbations, allowing a rapid adjustment of the experimental conditions in order to tune the material properties in real time.[41] Integration of chemical detection in the microfluidic system would enable high-throughput screening of the chemical process under controlled conditions, which is often difficult in conventional macroscopic systems.[39] Microstructured reactors offer also many opportunities for new production concepts by offering the possibilities to perform large numbers of independent chemical reactions for the purpose of synthesizing new compounds.[39, 42] Multiple process steps and/or parallel reactions can be integrated on a single chip with microfabricated networks with individually addressable microchannels and reservoirs.[43, 44] Continuous synthesis is believed to be one advantage of microreactor technology, which means the possibility of running up to 24h per day and doing analyses on line.[45] Especially, a multi-step continuous synthesis in a microreactor was expected to provide better quality functional products with improved economics for complicated reaction.[8] In a continuous-flow system, reactions are performed at steady state, making it possible to achieve better control and reproducibility.[46] Also, the ability to manipulate reagent concentrations in both space and time within the channel network of a microreactor provides an additional level of reaction control which is not attainable in bulk stirred reactors where concentrations are generally uniform. Furthermore, the spatial and temporal control of chemical reactions in microreactors, coupled with the features of very small reaction volumes and high surface interactions can be useful to control and alter chemical reactivity, relative to the situation of homogeneous solutions, in a rapid and efficient manner.[7]

Ali Abou-Hassan was born in Lebanon, He received his BSC and MSc degrees in chemistry from Pierre & Marie Curie university (UPMC, Paris 6). He completed his PhD work on using single phase flow microfluidics to study the synthesis and the fonctionnalisation of magnetic nanoparticles at PECSA Lab. in Pierre & Marie Curie university under the direction of Prof. Valérie Cabuil. Currently he is undertaking postdoctoral-research at Max Planck Institute for Colloids and Interfaces where he is working on the self-assembly of inorganic nanoparticles under the direction of Prof. Helmuth Möhwald.

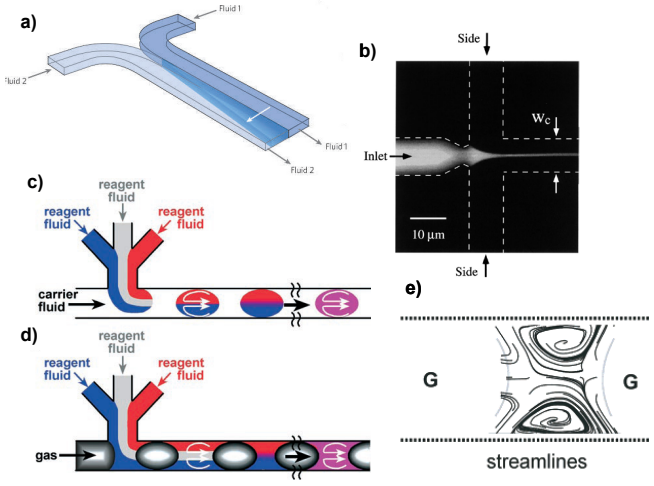

Figure 1. Some examples of different passive mixing techniques used in chemical synthesis. a) Mixing of two miscible fluid streams by flow lamination. The component streams mix only by diffusion, creating a dynamic diffusive interface with predictable geometry. Reproduced from ref [25], copyright Elsevier Science B.V., 2005. b) By hydrodynamic focusing of the inner stream (inlet) by an outer stream (side). Reproduced from ref [30], Copyright the American Physical Society, 1998. Encapsulated mixing in c) Discrete liquid plugs. d) Liquid slugs. Reproduced from ref [47], copyright Wiley-VCH Verlag GmbH & Co. KGaA., 2006. e) Recirculation streamlines in gas-liquid segmented flow. Reproduced from ref [32], copyright the American Chemical Society., 2005.

3. Microfluidics for liquid-liquid extraction of inorganic species

Separation is an important problem in chemical engineering and liquid-liquid extraction (LLE) even if it involves organic solvents, stays one of the most efficient techniques to selectively extract or separate neutral organic or inorganic species. Inorganic chemistry is mostly concerned by LLE, for example when heavy metals have to be eliminated from effluents, or when actinides or long-lived radionucleides have to be separated.[48] Usually metallic species are extracted from water to organic solvents after chelation or formation of ion pairs. Curiously, even if LLE is widely used and mastered, the transport of molecular or ionic species from one phase to another one through an interface is still not fully understood. The area of the interface is of course a key parameter. As microfluidics allows a major improve of the surface-area-to-volume ratio, it is mostly important to consider the use of microchips to improve or study the separation and extraction processes. This concept has been widely investigated by the group of Kitamori, who proposed a general methodology for the integration of all the usual unit operations of chemical engineering onto a microchip.[45, 49] He validated the idea to use glass microchips for studying molecular transport, namely the extraction of a Ni-dimethylglyoxime complex from water to a chloroform phase.[50] The chelates in organic solvent were quantified using the thermal lens microscope (TML), developed in his lab, allowing to localize even non fluorescent molecules.[51] When fluorescent complexes are extracted, as Al-DHAB (DHAB= 2,2 dihydroxyazobenzene) in organic phase, spatially resolved fluorescence spectroscopy can be used to study extraction. The concentration of Al-DHAB in the oil phase was thus mapped in the microchannel during extraction by 2,2 dihydroxyazobenzene and compared to simulations.[52]

Kitamori proved that extraction was possible in a microchannel, and found, for the extraction of a Fe(II) complex by a chloroform solution of 1-Octanaminium, N-methyl-N,N-dioctyl-chloride, an extraction time of the order of 45 s, that means about 20 times shorter than the extraction time in bulk (using mechanical shaking, Figure 2).[53] Coupling Micro Units Operations (MUOs), [45, 49] he coupled successfully in the same chip the synthesis of a complex (chelation of Co(II) by 2-nitroso-1-naphtol) and its extraction (in m-xylene).[54]

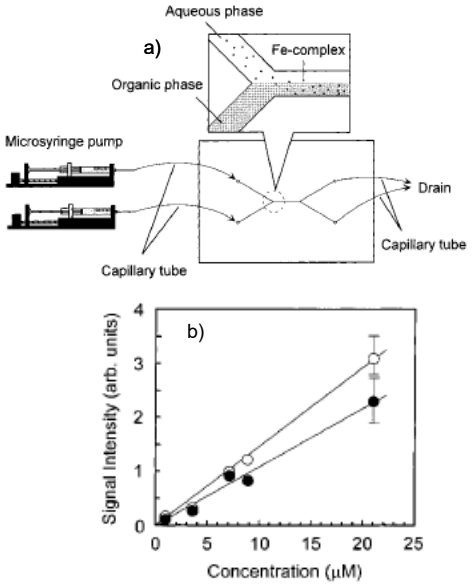

Figure 2. a) Schematic diagram of the integrated microextraction system. b) Dependence of the TLM signal intensity on the concentration of Fe(II) solution introduced: microchannel (●), separatory funnel (O). Reproduced from ref [53], copyright American Chemical Society, 2000.

In order to stabilize the interface, the length of the extraction zone was shortened and the angle made by the two liquids was reduced.[55] Another improvement was provided by fabricating intermittent partition walls at the center of the separation microchannel in order to successfully extract yttrium ions by 2-ethylhexyl phosphonic acid mono-2-ethylhexylester from an aqueous acidic mixture of Y^{3+} and Zn^{2+} ions. Flow analysis and modelling revealed that the partition induces a slight turbulence that promoted the extraction.[56] As the area of the interface is a key parameter for LLE, several methods inducing an increase of this area have been proposed. One solution is to produce stable multilayer flows in microchannels, as proposed by Hibara.[57]. This kind of chip was used to extract the aqueous Co-DMPA (Co-dimthylaminophenol) complex into m-xylene. The m-xylene was sandwiched in the central channel between the diluted aqueous solutions of cobalt complex (concentration of the order of 10-5 mol/L). The concentration of the complex in the m-xylene phase was measured using Kitamori's TLM. The extraction process in this three-layer flow system attained equilibrium about 3s after the contact, which has to be compared to the 60 s found in a diphasic configuration. Such a three-layer flow system was also used for the selective extraction of Yttrium by 2-ethylhexyl phosphonic acid mono-2-ethylhexylester as a liquid membrane separation system: the organic phase containing the extractant was sandwiched between the feed aqueous phase (an Y^{3+}/Zn^{2+} aqueous acidic mixture) and the receiving aqueous phase (a molar nitric acid solution). Y^{3+} selectively permeated through the liquid membrane within several seconds.[58]

In order to extract on the same chip different ions from an aqueous mixture, sequential pumping of different organic phases, each one of them containing an extractant specific of the ions to extract, was performed.[59] The concept was tested with extraction of Na^+ and K^+ cations and appeared to be efficient.

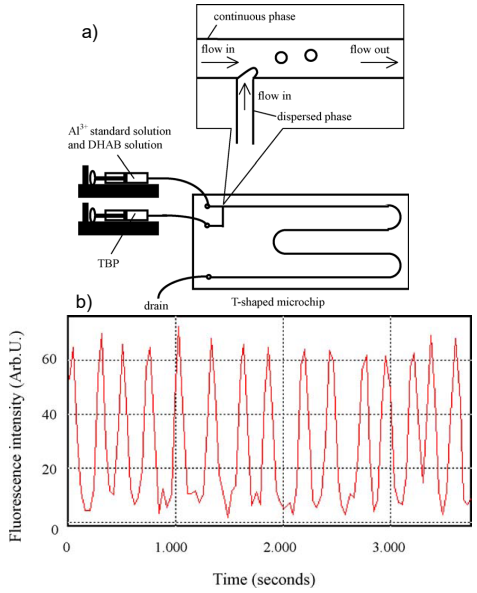

Figure 3. a) Schematic of droplet generation in T-shaped microchip. b) Fluorescence signal of Al^{3+}–DHAB in each droplet obtained at distance x = 53mm from confluent point. Flow rate of continuous phase: 37mms^{-1}. Flow rate of dispersed phase: 25mm.s^{-1}. The concentration of Al^{3+} solution was 80μg.L^{-1}. Reproduced from ref [60], copyright Elsevier B.V., 2006.

More recently, droplet based microfluidics was proposed to optimize liquid-liquid extraction (Figure 3).[60] The idea was again to extend the interface area, the latter being independent of the channel geometry, but easily controlled through the droplets size. Extraction of Al-DHAB complex from water to TBP (tributyl phosphate) was performed in a T-shaped microchannel, introducing the Al-DHAB complex as the continuous phase and the TBP as the dispersed phase. The efficiency of extraction was estimated from fluorescence measurements at several points of the channel. Again, extraction times appeared to be about 90 times shorter (of the order of 1 s) than times found in conventional methods. It was found that for the same specific interface area, extraction efficiency was not better in this configuration than in conventional devices; nevertheless, large mass transfer coefficients were obtained using such droplet based microfluidic compared to conventional mechanical shaking. A chip-based sequential-injection droplet array L-L extraction system was proposed more recently with chemiluminescence as an alternative to fluorescence for the detection of the extracted species.[61]

As a conclusion, it appears that in all cases microreactors (continuous flow or droplets ones) accelerate separation and allow strategies to take in charge selectivity for the extraction of inorganic cations. Results are less clear concerning enrichment factors that are not often explicitly discussed. On the fundamental point of view, microreactors can be used as convenient tools to investigate separation phenomena, explore selectivity of extractants and screen

their efficiency, of courses as soon as spectroscopic techniques, allowing a local characterisation of the species in the channel, are available.

4. Microfluidics for the synthesis of inorganic materials

We shall focus in the following section on the synthesis of inorganic nanoparticles in microfluidic devices. Indeed, it is the topic that has been mostly considered these last years in the field of inorganic synthesis. The main questions addressed are relative to the control of the size and shape of the nanoparticles and microfluidics has been considered as a possible technology allowing the investigation and the control of nanoparticle synthesis.

We first briefly remind the process for particles formation as explained by the classical nucleation theory (CNT) which occurs in the absence of a solid interface and consists in combining solute molecules to produce nuclei.[62] Three steps are usually considered: the nucleation, the growth (primary growth) and the aging (secondary growth). In the nucleation step, tiny particles precipitate spontaneously from a supersaturated precursor solution. When the precursors concentration falls down below the minimum concentration for nucleation, the latter stops, whereas the growth continues. Crystal growth occurs by addition of soluble species on the solid phase. In most cases, nucleation and growth occur concurrently throughout particles formation and the final particles therefore exhibit a broad size distribution. Besides, the size of the critical nuclei and the particles growth rate depend on the experimental conditions (concentration, temperature and pressure). Thus, to achieve a narrow size distribution, a short nucleation period (that generates all of the future particles) followed by a self-sharpening growth process and a constant chemical environment are required. Microreactors can be designed to meet these requirements, and a large number of microreactors have been reported for nanoparticle synthesis.

Three families of inorganic materials have been mainly studied: metals, metallic oxide and semiconductors. We shall begin this section by a short review of all the microreactors that have been used for the synthesis of inorganic nanoparticles. Then a paragraph will be devoted to each kind of materials under consideration. The last paragraph of the section will describe composites materials based on inorganic nanoparticles that have been obtained thanks to microfluidics.

Olivier Sandre graduated from the ESPCI Paris school of physics and chemistry in 1996. He received his PhD in 2000 from UPMC Paris 6 university at the "Physicochimie Curie" lab under the supervision of Prof. F. Brochard-Wyart. He spent one post-doctoral year in 2001 at UC Santa Barbara in the groups of Prof. D. J. Pine and Prof. D. K. Fygenson to study properties of biomaterials, before starting his career as CNRS researcher in the group of Prof. V. Cabuil at UPMC Paris 6 to elaborate new nanocomposite materials based on polymers and magnetic nanoparticles.

4.1 Microreactors for synthesis

Microfluidic reactors fabricated so far are made of glass, silicon, PDMS, stainless steel, ceramic, or SU-8.[28, 63-66] Glass is still a favourite material for the chemist, who is familiar with its chemical robustness and optical transparency. Silicon also has much to offer because of its electrical properties and compatibility with a multitude of fabrication processes, including the integration of electrical circuits. Depending on the final use and application, the materials with the best advantages are chosen, If high-temperature reactions (>200 °C) are carried out, glass-based microreactors are preferred. For applications at room temperature or up to 200 °C, polymer-based microreactors can be used, except if organic solvents are needed, as it is the case for Liquid-Liquid Extraction. Then glass is again preferred.

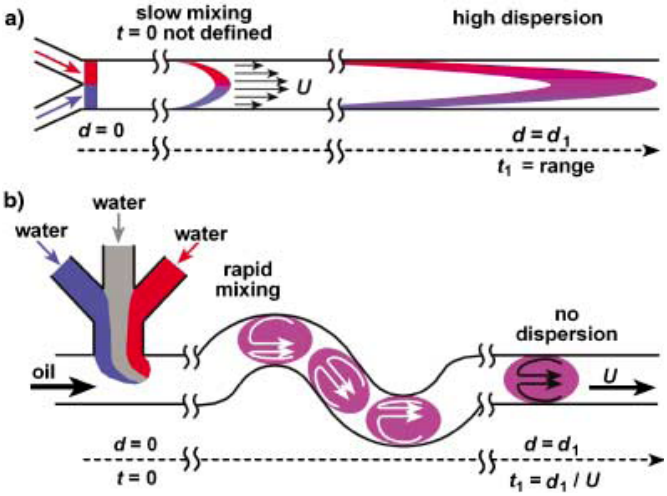

Figure 4. Schematic comparison of a reaction A+B conducted in a standard pressure-driven microfluidic system device (a) and in the droplets based microfluidic system (b). a) Reaction time t≠d/U. b) Reaction time t=d/U. Two aqueous reagents (red, A and blue, B) can form laminar streams separated by a gray "divider" aqueous stream in a microchannel. When the three streams enter the channel with a flowing immiscible fluid, they form droplets (plugs). The reagents come into contact as the contents of the droplets are rapidly mixed. Internal recirculation within plugs flowing through channels of different geometries is shown schematically by arrows. Reproduced from ref [31], copyright Wiley-VCH Verlag GmbH & Co. KGaA., 2003.

Both single phase continuous flow microreactors and emulsion (2-phase) micro droplets/segmented flow microreactors have been reported for the elaboration of nanomaterials. Continuous flow reactors have been widely used for synthesis due to their simplicity and operational flexibility.[67] Reagents mix and react under diffusion-based laminar flow reaction; reaction times, temperatures, mixing efficiency, and reagent concentrations are the typical control parameters for the synthesis of nanomaterials.[68] A significant problem encountered in single-phase microfluidic systems is the one of achieving rapid and efficient mixing of the fluids while minimizing the Taylor-Aris's dispersion effect caused by the parabolic (Poiseuille's) velocity profile (Figure 4a).[69] The latter is responsible for the large distribution of residence times that may cause significant variation in the yield, efficiency and product distribution of a reaction.[14] The confinement of reactions in nanoliter-sized droplets can serve as a method to overcome this problem.[47] In multiphase microfluidic reactors, reactants are compartmented into droplets or "plugs" effectively narrowing the

residence time distribution in both phases (Figure 4b).[31, 34]. In one common multiphase system, the continuous phase is oil that totally wets the walls of the microfluidic channel and the droplets are made of the aqueous synthesis mixture.[31] In the case of gas-liquid reactions or reactions in anhydrous solvents, gas-liquid segmented reactors have also been developed: in such reactors, the droplet phase consists of discrete bubbles of a gas within a liquid continuous phase.[32] Such reactors can be convenient for kinetic studies; for example Laval et al. recently developed a droplet based microfluidic system that allows to store the droplets on-chip and to control precisely their temperature in such a small volume.[70] It was possible to quantify by direct measurements the nucleation rate of KNO_3 precipitation in water, which seems to occur through heterogeneous mechanisms that involve impurities with different activities randomly distributed among the droplets up to supersaturation close to S=Ln(C/Csat)≈ 8.

4.2 Synthesis of semiconductors

Semiconductor (CdS, CdSe, ZnS…) nanoparticles, i.e. quantum dots, have been the first nanoparticles synthesized in a microfluidic device.[71] They are of considerable scientific and commercial interest owing to their tuneable optical and electronic properties, and potential applications in a wide range of electronic devices.[72] Physical properties of these nanocrystallites are strongly related to the physical size and shape of the crystallites. Indeed, there is a considerable interest in processing routes producing nanoparticles of well defined size.[73] The most successful and widely adopted QDs synthesis involves the injection of a liquid precursor into a hot bulk liquid, followed by growth at a lower temperature in the presence of stabilizing surfactants.[74] Controlling the conditions of such a process in bulk is difficult,[75] and microfluidics has thus been proposed as an alternative synthetic approach to control nanocrystals growth.[76] Indeed, the direct correlation between the QDs diameter and the UV-Visible absorption allows a rapid on-line particles size determination.[46, 76].

Microfluidic synthesis of CdS nanoparticles after mixing of $CdNO_3$ and Na_2S (in the presence of a sodium polyphosphate stabilizer) in a laminar microfabricated mixer[77] was first reported by Edel et al. in the DeMello group in 2002.[71] A broad range of crystallite sizes with an improved monodispersity (compared to bulk synthesis) was obtained by increasing the residence time of the reagents.

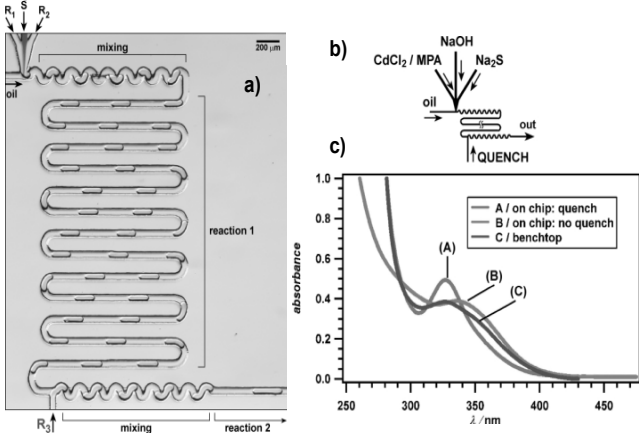

Figure 5. Micrograph of a PDMS microfluidic device used for performing droplet based synthesis of nanoparticles; b) Two-step synthesis on chip with millisecond quenching yields CdS colloidal nanoparticles that are less disperse than those synthesized on chip; c) UV/Vis spectra of nanoparticles synthesized on chip with millisecond quench (A), on chip without quench (B), and on the bench top (C). Reproduced from ref [78], copyright Royal Society of Chemistry, 2004.

As laminar reactors are subjected to Taylor dispersion and clogging, Shestopalov et al.[78] isolated the reaction inside aqueous droplets, that were surrounded and transported by a fluorocarbon oil immiscible with water (Figure 5). Aqueous droplets containing $CdCl_2$, mercaptopropionic acid (MPA), Na_2S and NaOH solution were formed within 5 ms into the oil flow. The control of the CdS particles (and of core/shell CdS/CdSe nanostructures) was improved when the microreactor was used. Later on, always in order to reduce technical problems, increasing the mixing time and lowering the dispersion effect, Hung et al. proposed a microfluidic device that can alternately generate droplets and fuse them under a velocity gradient in an expansion chamber (Figure 6). [79]

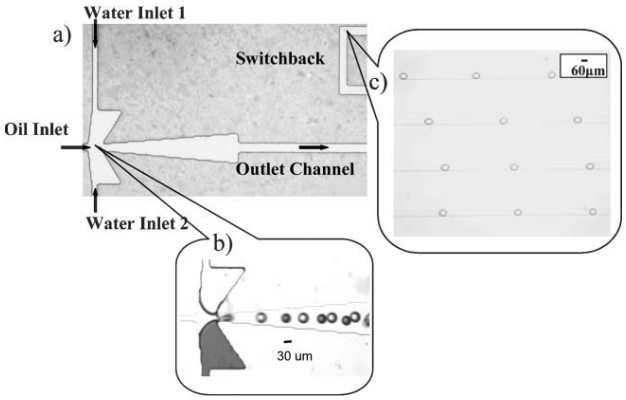

Figure 6. a) Microscope image of the PDMS channel magnified at the doublet T-junction channel; b) Water-in-oil alternating microdroplet generation. Green dye is added into water inlet 2 for the differentiation purpose; c) Fused droplets align in the long switchback channel. Reproduced from ref [79], copyright Royal Society of Chemistry, 2006.

Fundamental investigation of the reaction process was reported by Sounart et al. who synthesized in a continuous-flow microfluidic reactor cysteine stabilized CdS nanoparticles and studied in-situ by spatially resolved photoluminescence imaging and spectroscopy the particles growth.[80] Their results provided a direct insight into the kinetics and the mechanistic data of the QDs formation.

CdSe nanoparticle synthesis has also been extensively studied.[32, 46, 76, 81-84] In the initial experiments described by Nakamura et al. CdSe QDs synthesis was performed continuously within a fused silica capillary (200- 500 µm id) immersed in an oil bath, at temperatures ranging from 230 to 300°C and with reaction residence times determined by the volumetric rates and the capillary dimensions.[81] Large nanoparticles were obtained by increasing respectively the temperature or the residence time. To minimize the distribution of the residence times generated by hydrodynamic pumping of fluids through the microchannel, the authors segmented the reaction solution with nitrogen bubbles at defined intervals. A more detailed study of size-controlled growth of CdSe nanoparticles in microfluidic reactor has been reported by Chan et al.[76]. A heated microfabricated borosilicate glass chip-based reactor was used for the continuous high temperature synthesis, control and characterization of CdSe nanocrystals. Dimethyl cadmium was mixed with selenium dissolved in boiling tri-octylphosphine (TOPO) and octadecene (ODE) in the microfluidic reactors and the effect of the temperature, flow rate, and concentration of precursor in solution (all these parameters being varied independently) was studied. For example, increasing the temperature resulted in an increase of the particles size and a narrowing of the size distribution. Outgassing and clogging are usual problems encountered during the

synthesis within microreactors at high temperatures. Yen at al. [46] avoided the problem by using appropriate chemical reagents. Cadmium oleate and TOP-Se complexes were dissolved in a high boiling point solvent system consisting of squalane, oleyl amine and TOP. The synthesis was carried using a continuous flow reactor with a miniature convective mixer followed by a heated glass reaction channel maintained at a constant temperature (180-320°C). The authors elegantly showed the possibility to finely tune the size of CdSe nanocrystals produced in the reactor by systematically varying the temperature, the flow rate and the concentrations. Later the same group reported the use of a gas-liquid segmented flow reactor with multiple temperature zones for the synthesis of high quality CdSe quantum dots.[32] The reactor designed allows rapid mixing of the precursors and on-chip quenching of the reaction. The authors compared their results to those obtained in the continuous flow method and concluded that the enhanced mixing and narrow residence time distribution characteristic of the segmented flow reactor resulted in a significant improvement of the reaction yield and of the size distribution, especially for short reaction times during the synthesis of CdSe nanoparticles.

Synthesis at high pressure and temperature of CdSe nanoparticles in a continuous microfluidic reactor was recently reported by Marre and coworkers.[84] They carried out the synthesis using either squalane or supercritical hexane as a solvent (Figure 7). The synthesis in hexane (liquid or supercritical) resulted in a decrease of 2% in the size distribution of the QDs due to a decrease of the residence time distribution caused by its lower viscosity compared to squalane. Most notably, the use of supercritical hexane led to higher supersaturation compared to squalane, producing a larger number of nuclei thus narrowing the size distribution of QDs.

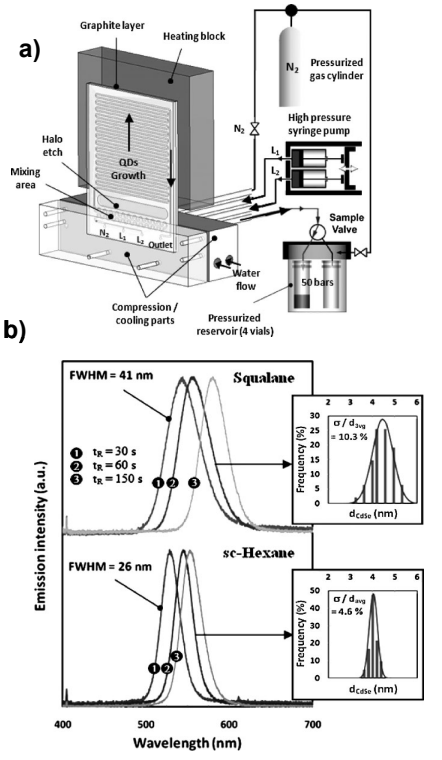

Figure 7. a) Schematic of the experimental set-up used for the synthesis of QDs. The microreactor consisted of a 400 µm wide and 250 µm deep channel with a 0.1 m long mixing zone maintained at room temperature and a 1 m long reaction zone heated up to 350 °C. The two zones were separated by a thermally isolating halo etch that allowed for a temperature gradient of over 25 °C mm^{-1}. The entire set-up was first pressurized from the inlet to the outlet using a nitrogen gas cylinder. Thereafter, the nitrogen valve was closed and the two precursor solutions were delivered independently using a high pressure syringe pump, insuring good control of the flow rate. b) Photoluminescence spectra at different residence times (t_R) obtained for CdSe QDs synthesized in squalane and hexane at 270 °C, 5 MPa with [Cd] = [Se] = 3.8 x 10^{-3} M and QD-size distribution obtained from TEM measurements for samples run at t_R = 60s. Reproduced from ref [84] copyright Wiley-VCH Verlag GmbH & Co. KGaA., 2008.

Temperature gradients can be also used to induce a better control over the nucleation and growth of the nanoparticles and narrow the size distribution. Steep temperature gradients were created in a heating section of a microreactor designed to induce burst nucleation of CdSe in its high temperature zone and to promote growth in its low temperature zone (Figure 8).[85] The superiority of this two-temperature approach on the kinetic control of the QDs was demonstrated as the synthesised nanoparticles exhibited higher nuclei concentration and narrower size distribution.

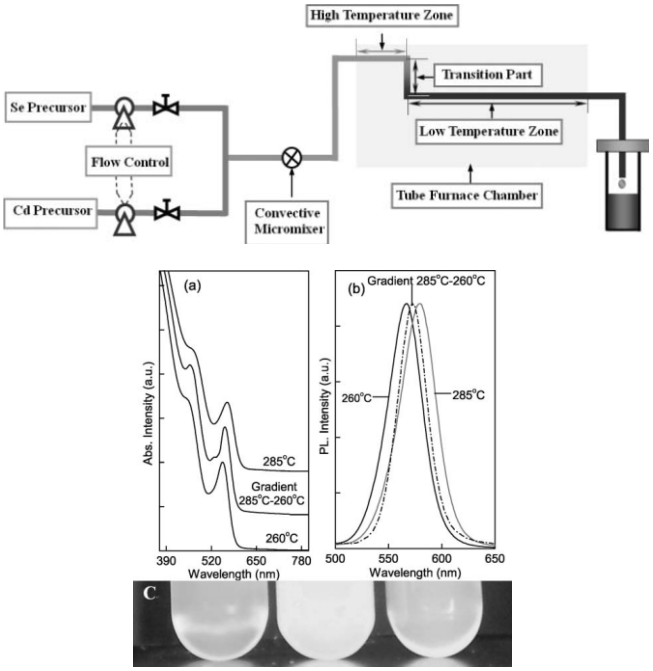

Figure 8. Up; Process map for the synthesis of CdSe QDs in a capillary microreactor with two-temperature approach in the heating section. The microreactor consisted in a convective mixer placed before a capillary tube (300µm id). The latter was formed of three different parts whose lengths can be varied: (i) a high temperature zone to induce burst nucleation, (ii) a transition zone and (iii) a low temperature zone to promote growth of the nanoparticles. Down ; (a) Absorption spectra and (b) Photoluminescence spectra of the samples produced using using the two-temperature approach and the constant temperature approach cia microreaction with the the same residence time; (c) Emission from the three samples with the same absorption value at 365 nm under 365 nm UV light (from left to right: 260 °C, 285-260°C, 285°C). Reproduced from ref [85], copyright Royal Society of Chemistry, 2008.

Synthesis of doped semiconductor nanoparticles in microfluidic devices has also been reported. Singh et al. investigated the synthesis of 1-thioglycerol-capped Mn-doped ZnS nanocrystalline semiconductor nanoparticles via a microfluidic approach at room temperature and at 80 °C.[86] Photoluminescence, X-ray photoelectron spectroscopy, atomic absorption spectroscopy and electron paramagnetic resonance studies confirmed the presence of Mn^{2+} in the ZnS nanoparticles.

The stability and properties of QDs are improved by coating the semiconductor cores (CdS, CdSe) by a nanometric shell (even two) of another semiconductor as ZnS.[87] The thickness of the ZnS shell is crucial to obtain high quantum yield of the ZnS-capped CdSe QDs[88, 89] and microfluidics appears very promising to perform such a controlled coating. Wang et al reported the first multi-step continuous-flow method for the synthesis of ZnS-coated CdSe QDs using microfluidic reactors.[90] UV-Vis spectra showed that CdSe particles and the ZnS coating were produced consecutively. The particles size and the layer thickness were directly adjusted by the flow rate. In another work, the same authors focused their study on the optimization of the coating step, by using in the same microreactor as the one described above and a single molecular source $[(C_2H_5)_2NCSS]_2Zn$ that has a low toxicity and a good stability in the air.[91] The effects of the residence time, of the CdSe core size and of the temperature on the final coating and on the photoluminescence quantum yield (QY) were investigated by absorption and photoluminescence spectroscopy. Fluorescence QY above 50% was obtained when an optimized residence time was chosen in the microreactor. QY remained high even when the nanocrystals surface was modified to be hydrophilic. Recently, a facile method based on microfluidic for the synthesis of CdSe/ZnS core shell structures with pure green luminescence involving short residence time and low reaction temperature (t = 10 s, T = 120 °C) was proposed by Luan.[92] CdSe nanoparticles and Zn sources were mixed by a convective mixer before entering a heated PTFE capillary for the coating process. As the temperature for the coating step was low, the synthesis of the core shell nanoparticles was continuous and did not require any purification of the CdSe nanoparticles. Homogeneous coatings of ZnS were achieved with fairly wide operation parameters (residence times, temperatures…). The synthesis of ZnS/CdSe/ZnS particles using microfluidic reaction technology was also explored.[93] Thanks to the homogeneous and accurate control of heating temperature and time in a microreactor, the true epitaxial deposition of CdSe monolayers onto the ZnS nanocrystals was possible despite the lattice mismatch between ZnS and CdSe. The fluorescence wavelength and the quantum yield of these nanoparticles were tuned by controlling the flow rate during the CdSe layer deposition step.

Valérie Cabuil is full professor at Pierre & Marie Curie university (Paris 6) since 2001. She is director of a laboratory involved in colloidal science and physical chemistry (PECSA Lab.) and of a doctoral school devoted to physical and analytical sciences.

Her research deals with inorganic nanoparticles, especially magnetic ones, their synthesis, modification and colloidal stability. She recently introduced microfluidics in her team for the synthesis and modification of inorganic nanoparticles.

4.3 Synthesis of oxide nanoparticles

Oxide nanoparticles are widely used and described. They can be obtained through several procedures, some of them being easily transposable in microfluidic devices. [44, 94-101].

Wang et al. obtained TiO_2 nanoparticles from the hydrolysis and condensation of titania tetraisopropoxide (TTIP) at room temperature using the stable interface obtained with the appropriate flowing rates and viscosities ratios between two insoluble laminar flows in a microchannel reactor.[94] The authors described the water/oil interface as a novel type of "nano-like" reaction chamber and expected special characteristics to be obtained assuming that the particle growth mechanism at the interface of immiscible flows may be different from that in beakers. TiO_2 colloids were collected at the outlet of the microreactor and characterized off-line using UV/visible spectra and TEM images, which confirmed the presence of the TiO_2 anatase polymorph. Based on the same idea of conducting reactions at the interface of two immiscible liquids and in order to avoid the precipitation of the particles at the walls, Takagi et al. developed a microreactor with double-pipe structure [95] Two immiscible liquids were respectively flowed in the inner and outer tubes and maintained an annular and laminar flow of two separated phases that create a microspace delimited by the outer fluid wall. The inner flow acted as a microchannel which radius can be varied by the operating conditions. The particles produced that way at room temperature were mono-modal spherical particles of amorphous titania with a narrow size distribution compared to the random size distribution obtained in a conventional batch method. Besides, it was possible to control the particles size in the range from 40 to 150 nm only by changing the diameter of the inner tube at a low TTIP concentration.

Khan et al. studied the influence of the reactor design and of parameters as the linear flow velocity and the mean residence times, on SiO_2 particle size distribution.[98] The particles were obtained using the so-called Stöber's process.[102] Two reactor configurations were examined: laminar flow reactors and segmented flow reactors (Figure 9). As laminar flow reactors are affected by axial dispersion at high linear velocities, wide size distributions of the colloidal SiO_2 were observed. In segmented flow reactors the internal backflows, created inside the liquid plugs, generated mixing, which eliminated the axial dispersion effects and produced a narrow size distribution of silica nanoparticles.

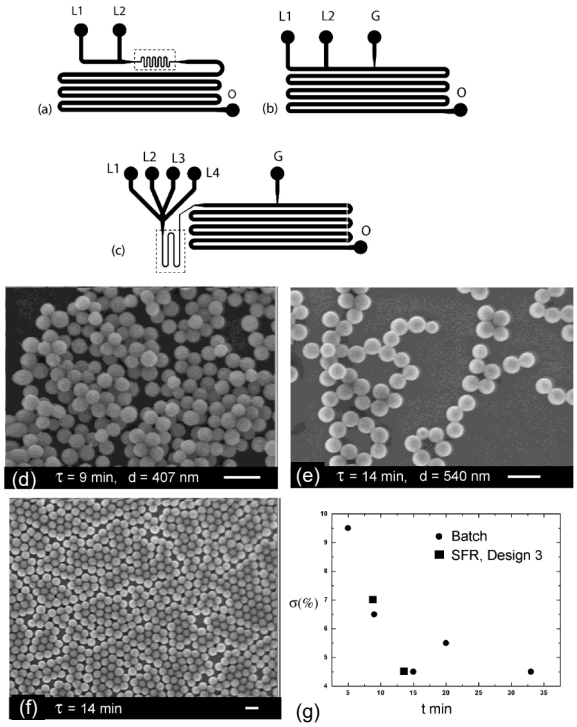

Figure 9. Schematics of microfluidic channels: (a) Design 1 (LFR) has two liquid inlets (L1 and L2) and one outlet (O). (b) Design 2 (SFR) has two liquid inlets (L1 and L2), a gas inlet (G), and an outlet (O). (c) Design 3 (SFR) has four liquid inlets (L1-L4), a gas inlet (G), and an outlet (O). Segmented flow reactor (SFR, design 3). Sequence of SEM micrographs corresponding to various residence times: (d) 9 min; (e) 14 min (f) low magnification SEM of sample (e), the organization of particles into pseudocrystalline domains is an indicator of the high monodispersity of the microreactor product; (g) graph of standard deviation (σ) expressed as a percentage of mean diameter versus residence time (t min) in the SFR as compared to batch reactor data. In all SEM micrographs, the scale bar corresponds to 1 μm. Reproduced from ref [98], copyright American Chemical Society, 2004.

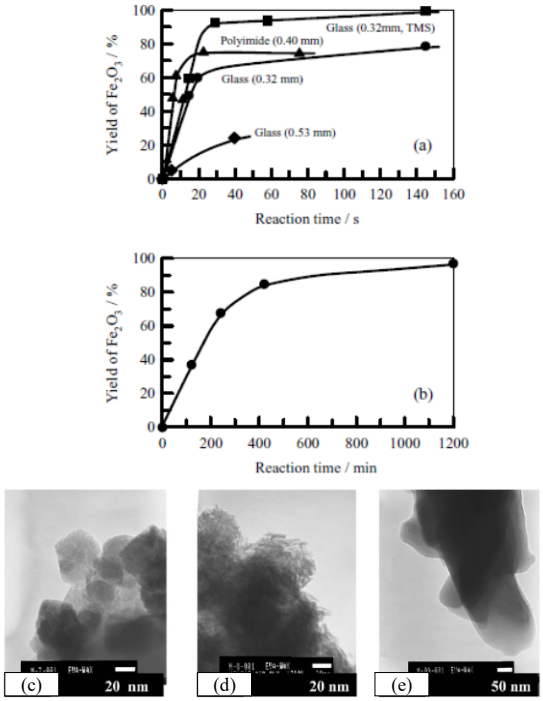

Figure 10. Influence of the reaction time on the yield of α-Fe2O3 (a) capillary tube reactors (b) autoclave (50 ml). TEM images of the products (a) glass capillary, (b) glass capillary (TMS) and (c) autoclave (50 ml). Reproduced from ref [101], copyright Springer, 2005.

Ferric oxides have also been synthesized in microreactors. Decomposition of $Fe(NO_3)_3$ in formamide at 150 °C was performed in microreactors consisting in capillary tubes of same or different inner diameters, made in glass, treated with trimethylsilyl chloride (TMS) and polyimide, all immersed in an oil bath maintained at 150 °C.[101]. A conventional autoclave was also used for comparison. Haematite nanoparticles α–Fe_2O_3 with different shapes were obtained depending on the microreactor. A comparison of the surface area of the reactor normalized by the reactor volume indicated an acceleration of the reaction when the specific area was increased.

The continuous microsynthesis of stable magnetite nanoparticles Fe_3O_4 by coprecipitation of an aqueous solution of a stoechiometric mixture of iron (II) and (III) salts by an alkaline medium was reported by our group.[99] The reactor consisted in a coaxial flow microreactor as the one reported by Takagi et al. for the synthesis of TiO_2 nanoparticles.[95] The outer capillary was obtained by molding in PDMS (1.6 mm id) and the inner one was a glass capillary of 150 μm inner diameter. The flow rates of the miscible liquids were continuously varied in order to achieve fast mixing and different residence times. At the outlet of the reactor, the reaction was quenched by solvent extraction in cyclohexane using a surfactant. The superparamagnetic behaviour of the nanoparticles and their spinel structure were confirmed respectively by vibrating sample magnetometry (VSM) and electron diffraction. From the VSM measurements, it was concluded that the nanoparticles produced within a few second in the channel presented a narrow size distribution below the typical values obtained by the batch coprecipitation and exhibited a small decrease of ordering of their magnetic moments.[103] Later on, the same setup was improved by separating a nucleation reactor and an aging channel in order to synthesize antiferromagnetic ferrihydrite α–FeOOH nanolaths. [44] In the nucleation microreactor, ferrihydrite nanoparticles were precipitated by fast mixing of $FeCl_3$ and an alkaline solution of tetramethylammonium hydroxide (TMAOH). The suspended ferrihydrite nanoparticles were directly injected from the outlet into a microtubular aging coil (1.7 mm id) continuously heated in a water bath at 60 °C. TEM and HRTEM images confirmed the acceleration in the aging process of the ferrihydrite phase into goethite: plate-like nanostructures of goethite were detected after only 15 min of continuous aging in the microreactor, while several hours are necessary in batch conditions. Droplets-based synthesis of magnetic iron oxide nanoparticles was also reported by Frenz et al.[100] The authors designed a microfluidic reactor that enabled to generate droplet pairs based on hydrodynamic coupling of two spatially separated nozzles (Figure 11). One of the droplets contained the iron

mixture while the other one contained the ammonium hydroxide solution. When an electrical field was applied between the two on-chip electrodes, the droplet pairs coalesced and a precipitate of iron oxide nanoparticles appeared. The nanoparticles size measurements by TEM showed that the average particle diameter was smaller for the fast microfluidic compound mixing (4 ± 1 nm) than for bulk mixing (9 ± 3 nm). The absence of hysteresis in the magnetization curve and the high resolution TEM images confirmed the iron oxide spinel structure.

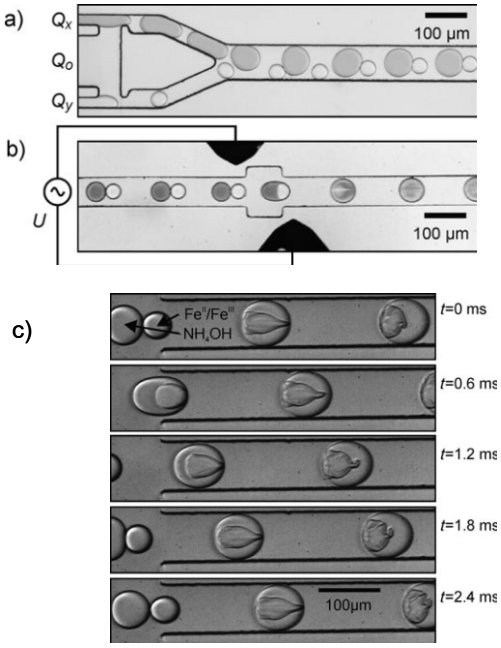

Figure 11. a) Pairing module. Two aqueous phases are injected by the outer channels and are synchronously emulsified by the central oil channel. b) Fusion module. Paired droplets can be coalesced by applying an electrical voltage U between the two electrodes. c) Formation of iron oxide precipitates after coalescence of pairs of droplets. Reproduced from ref [100], copyright Wiley-VCH Verlag GmbH & Co. KGaA., 2008.

As it was the case for quantum dots, core-shell oxide nanoparticles have also been synthesized in microfluidic devices. Khan et al. developed, for the coating of colloidal SiO_2 by TiO_2 , a continuous-flow microreactor allowing a controlled multi-point addition and mixing of a reactant to a primary feed (Figure 12).[104] The segmented gas-liquid flow coating device enabled the multi-step addition through a branched manifold and the rapid mixing of small amounts of titanium tetraethoxide (TEOT) throughout the process, yielding to coatings of controlled thickness. When the TEOT was added in a single step to a relatively monodisperse silica particles suspension, a polydisperse mixture of primary coated particles, secondary titania particles and large agglomerates were observed. On the contrary, when the branched manifold was used to feed the TEOT solution, the monodisperse nature of the initial particles population was preserved and both the secondary particle formation and agglomeration were avoided. After calcination at 500 °C, the core-shell nature of the particles was evidenced by TEM images which showed that the coating was composed of compact grains of titania deposited onto the primary silica surface. The microfluidic approach also allowed the tuning of the particle size by varying the addition rate of TEOT.

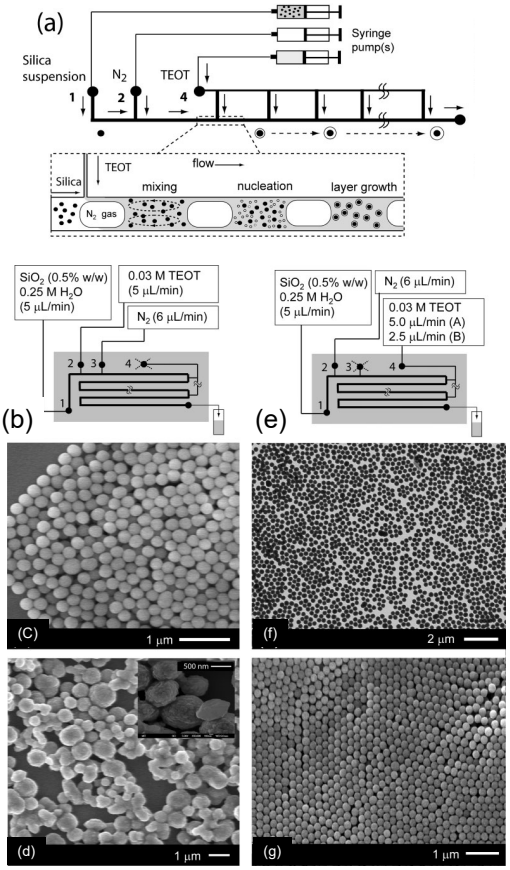

Figure 12. a) Design concept for continuous-flow coating reactor. b) Schematic view showing details of the single-step TEOT addition experiments. The branched manifold was not used in this case. c) SEM of silica particles used for the coating experiments (average diameter = 209 nm, standard deviation (σ = 11 nm). d) SEM of particles obtained from the single-addition experiment. Inset shows a high magnification SEM of the particle surface. e) Schematic view showing details of the multistep TEOT addition experiments. The branched manifold was used in this case. f) Low-magnification TEM of coated particles. g) SEM of coated particles after calcination at 500 °C. Reproduced from ref [104], copyright Wiley-VCH Verlag GmbH & Co. KGaA., 2007.

In our group, we also reported on the multistep continuous-flow synthesis of magnetic and fluorescent core shell γ-Fe_2O_3/SiO_2 nanoparticles by using several flow-focusing microreactors.[87] Three microreactors were connected in series, each one acting as a micro-unit for a defined operation. The first microreactor enabled the grafting of (3–aminopropyl) triethoxysilane (APTES) on the surface of γ-Fe_2O_3 nanoparticles previously coated by citrate ligands. The second microreactor enabled the fast mixing of the modified magnetic nanoparticles with the fluorescent silica shell precursors TEOS and APTES labelled with the fluorescent dye rhodamine B isothiocynanate. The final microreactor served for the hydrolysis-condensation reaction of the silica precursors catalysed by NH_3 onto the magnetic nanoparticles. TEM images confirmed the acceleration of the coating process as core-shell structures were observed after only 7 minutes compared to several hours in a conventional bath process. In addition, fluorescent chain-like structures were observed by fluorescence microscopy in the presence of a magnetic field, thereby evidencing the bifunctional character of the nanoparticles (Figure 13c).

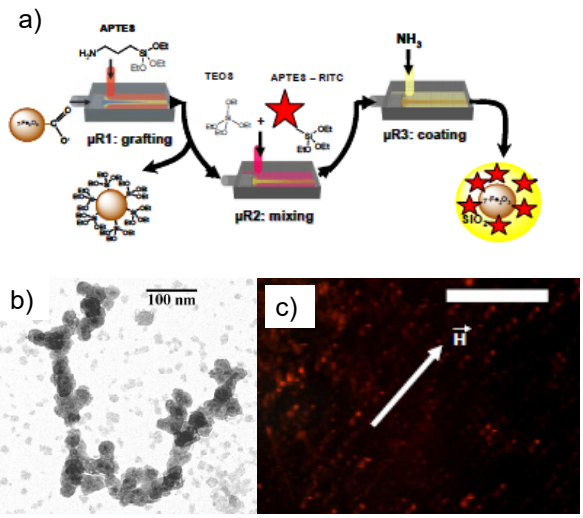

Figure 13. a) Cartoon of the coaxial flow microreactor (μR) used in this study showing the mixing between the inner stream (Q_{in}) and the outer stream (Q_{out}) b) Scheme for the continuous synthesis of fluorescent core-shell MNPs/Silica nanoparticles. μR1 = microreactor for APTES grafting on the citrated γ-Fe_2O_3 nanoparticles; μR2 = microreactor for mixing of the sol-gel precursors TEOS and APTES-RITC; μR3 = microreactor for coating of the γ-Fe_2O_3 nanoparticles with silica; APTES = (3–aminopropyl) triethoxysilane; TEOS = tetraethyl orthosilicate; RITC = Rhodamine B isothiocyanate. b) TEM micrographs showing typical architectures of the core-shell MNPS@SiO_2(RITC) nanoparticles. c) Fluorescence microscopy images of silica-coated iron oxide nanoparticles in the presence of an external magnetic field showing the formation of chain-like structures. Scale bar length: 50 μm. Reproduced from ref [87] copyright Wiley-VCH Verlag GmbH & Co. KGaA., 2009.

4.4 Synthesis of metallic nanoparticles

The optical, electronic and thermal properties of metallic nanoparticles endow them with potential applications in electrical and nonlinear optical devices,[105] improved dielectric materials,[106] nano-materials for bio-imaging or hyperthermia[107] and high thermal conductivity "nanofluids".[108] Synthesis of Au, [109-114] Ag ,[32, 115] Cu,[116] and Pd[117] nanoparticles in microfluidic reactors were reported. Due to their greatly enhanced light absorption (Mie scattering) at the plasmon resonance wavelength,[118-120] the growth and shape of metallic nanoparticles can be monitored optically, thus offering a convenient system to be studied in microfluidic devices.

Wagner et al. reported on the synthesis of 15 to 24 nm spherical Au nanoparticles, at room temperature, in a chip-based diffusion microreactor following a seeding growth approach.[109] To initiate the growth of larger Au nanoparticles, the microsynthesis started from 12 nm citrate-stabilised gold seeds, which were conventionally synthesized out the microsystem. Ascorbic acid was used as a soft reducing agent of $HAuCl_4$ at the surface of the 12 nm seeds, serving as nuclei of the final particles, the latter being stabilized against aggregation by polyvinyl pyrrolidone (PVP). Off-line techniques (analytical centrifugation and AFM) enabled to deduce a mean particles diameter that was larger when the flow rate decreased. Later on, the same authors used a continuous flow microreactor for the synthesis of gold nanoparticles (5 to 50 nm) by reducing the gold precursor $HAuCl_4$ by ascorbic acid in the presence of PVP.[110] Several parameters as the flow rate, the pH, the reagents concentrations and the PVP concentration were screened. The surface modification of the microsystem in order to avoid fouling and adsorption of the nanoparticles onto the microreactor walls was also examined. In the end, this microfluidic device produced gold nanoparticles with a size distribution width twice as narrower than the one obtained in a conventional synthesis.

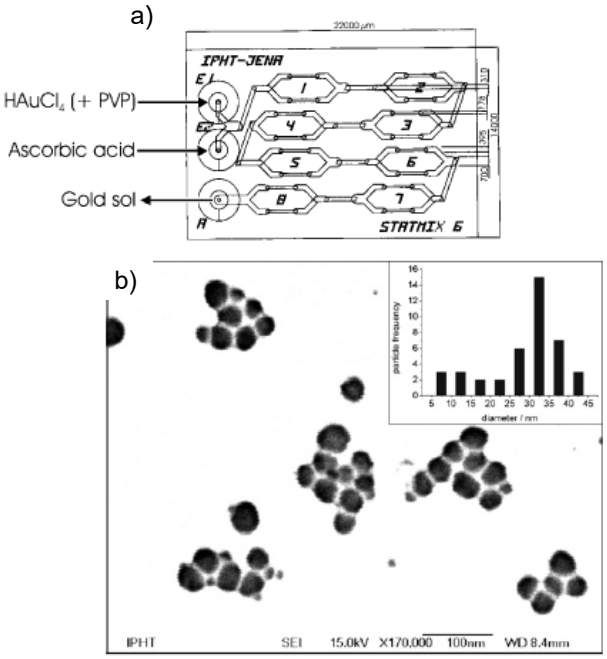

Figure 14. a) Schematic drawing of the experimental setup showing the connectivity of the IPHT microreactor (STATMIX 6, area 22 X 14 mm). b) SEM image (with particle size analysis as inset) of gold particles obtained at a flow rate of 500 μL/min (native reactor, pH) 2.8, 1 mM HAuCl4, 20 mM ascorbic acid, 0.025% PVP). Reproduced from ref [110], copyright American Chemical Society, 2005.

To obtain very small gold nanoparticles, the same authors used borohydride $NaBH_4$ as a stronger reducing agent during the synthesis in the microfluidic reactor.[113] This reducing agent and the same microreactor were also used for the synthesis of Ag nanoparticles from $AgNO_3$ precursor, followed by a direct surface modification with thiol ligands. The direct reduction of $HAuCl_4$ with $NaBH_4$ produced gold nanoparticles with a diameter ranging between 4 and 7 nm reproducibly. In the investigated flow rate range, no variation of the particles size distribution was observed when the flow rate was varied. The same behaviour was observed when the concentration ratio of the precursor to the reducing agent and the pH was varied. Concerning silver nanoparticles, their mean diameters were much larger (~ 15 nm). Even though the mean particles size of the silver nanoparticles was nearly unaffected by the flow rate just as for gold, the size distribution width was lowered by either increasing the flow rate or increasing the $NaBH_4/AgNO_3$ ratio, in contrast to what was observed for gold nanoparticles. The same group also reported on the synthesis in microreactors of bi-metallic nanoparticles with various compositions of silver and gold for catalytical applications. They showed that the optical properties of the colloidal product solutions were affected by the mixing order of the reactant solutions and the overall flow-rates. Microfluidic continuous flow synthesis of rod-shaped gold and silver nanocrystals was described by Boleininger et al.[112] They adapted the synthesis method originally described by Nikoobakht et al.[121] and Jana et al.[119] to a microfluidic process. Conventionally the method is based on the growth of metal nanorods from spherical metal seed crystals in an aqueous "growth solution" containing the $HAuCl_4$ or $AgNO_3$ precursors, a soft reducing agent as ascorbic acid and a high concentration of a surfactant molecule as CTAB. The microreactors used in this study consisted in a capillary tube made

in PVC (1 mm id) for the gold nanorod synthesis and in PEEK (0.75 mm id) for the silver nanorod synthesis, both immersed in a heat bath maintained at 30 °C The UV-Vis spectra (optical extinction) of the final product were measured at the outlet of the reactor by a flow-through spectrometer to approximate the aspect ratio of the nanorods. The effect of the ratio of growth to seed solution (*r*) and, of temperature on the final particles was investigated.

Thermal reduction of silver pentafluoropropionate in the presence of trioctylamine (TOA) as a surfactant, in isoamyl ether was reported by Lin et al. as a method for the synthesis of silver nanoparticles in a continuous flow tubular microreactor.[115] Unlike the commonly used methods for producing silver nanoparticles from silver salts in aqueous solution, the thermal reduction method described by the authors was a single phase system, suitable to generate narrow size dispersions. The synthesis mixture was introduced into a tubular coil, made of a stainless steel needle (0.84 mm id), heated to the designed temperature between 100 and 140 °C using an oil bath (Figure 15). The ratio TOA/silver pentafluoropropionate, the flow rate, the temperature vs. time profiles and the reaction temperature of the reactor were varied to investigate their effects on the average size and distribution width of Ag nanoparticles. Oleylamine was used as a capping agent to stabilize the nanoparticles at the outlet of the reactor before they were analyzed by TEM and off-line UV-Vis spectra. The change in the TOA concentration did not induce any substantial difference in either the size or size distribution of the nanoparticles, while an increase of diameters of the nanoparticles and of their polydispersity was observed when the flow rate was increased. He et al.[32] further studied the effect of the nature of the capillary tube on the synthesis of Ag nanoparticles. Their results indicated that a high affinity between the particles and the interior wall of the tube resulted into a broader size distribution and a lower production yield. Another method based on the principle that a metal ion M^{n+} or ion complex can be reduced to its atomic state M^0 by another metal with a lower redox potential was reported by Wu et al. for the synthesis of Ag nanoparticles.[122] The authors used different metal foils (Ni, Fe and Co) as heterogeneous reducing media and reactors to reduce $AgNO_3$ into Ag colloids. The particle size and size distribution could be tuned depending on the metal foil and on the residence time. Fine silver halide nanoparticles synthesis AgX (X = Cl or Br) in an annular multi-lamination microreactor was reported by Nagasawa.[123] They successfully achieved a stable and continuous synthesis without any clogging of the microchannel by flowing inactive fluids in the outermost and innermost annular streams. The influence of different operational parameters as the volume flow rates of the inactive fluids and the flowing solution in the middle stream on the particle size was investigated.

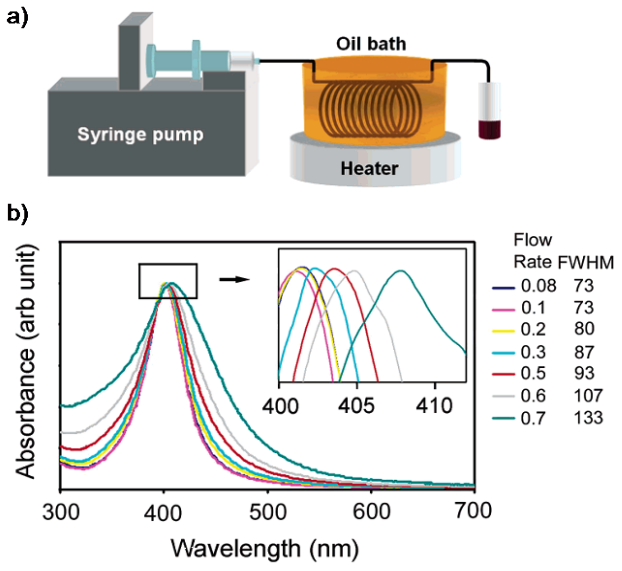

Figure 15. a) Experimental setup of the synthesis of Ag nanoparticles in a tubular microreactor. b) UV-Vis absorption spectra of silver nanoparticles made at the different flow rates. Instes show the enlarged peak region and a summary of FWHMs of the absorbance of the Ag nanoparticles (nm) at the various volumetric flow rates (mL/min) used. Reproduced from ref [115], copyright American Chemical Society, 2004.

The synthesis of size-controlled Pd nanoparticles was evidenced by Song et al using a polymer-based microfluidic reactor.[117] The polymeric continuous-flow microreactor was fabricated using a negative photo resist SU-8 on a 10 x 10 cm^2 polyetheretherketone (PEEK) substrate by standard UV photolithography. The Pd nanoparticles were synthesized by reduction of $PdCl_2$ by $LiBEt_3H$ in THF. The nanoparticles were characterized by TEM, selected area electron diffraction (SAED) and X-ray diffraction. The Pd nanoparticles synthesized in the microreactor were found to have a narrower size distribution when compared with those obtained by a conventional batch process. The same authors also reported on the synthesis of copper nanoparticles.[116] Compared with those produced by the conventional batch process, the Cu nanoparticles formed in microfluidic devices were smaller (8.9 nm vs. 22.5 nm) with a narrower size distribution and an improved stability versus oxidation. Cobalt nanoparticles were synthesized in a microfluidic reactor with three different crystal structures – face-centered cubic (FCC), hexagonal closed-packed (HCP) and ε-cobalt – according to the reaction times, the flow rates and the quenching procedures.[47] Zinoveva et al. probed the cobalt nanoparticle formation at three different positions in a PMMA microreactor using synchrotron-radiation-based X-ray absorption spectroscopy.[124] Co-K edge XANES spectra recorded at three different positions of the microchannel together with reference spectra of the precursor and the final product collected at the end of microfluidic system showed that a time resolution of the reaction of the order of milliseconds can be obtained from the spatial resolution within the microreactor, evidencing the power of the position-time equivalency in continuous-flow microfluidics.

4.5 Microfluidics for advanced materials science

As described above, the confinement and mass transport phenomena associated to microfluidics are well suited for the controlled synthesis and modification of inorganic nanoparticles. Microfluidic environments are also extremely promising for the controlled aggregation or encapsulation of inorganic nanoparticles in order to produce higher order structures, usually microscopic ones, with multifunctional properties.

4.5.1 Self-assembly of colloids

Three dimensional assemblies of monodisperse colloids have received much attention, primarily because of their potential as optical materials as photonic crystals for example.[125, 126] Similar to semiconductors in electronic devices, these photonic crystals can exhibit optical insulating behaviour due to a photonic bandgap (PBG).[127, 128] The controlled preparation of colloidal photonic crystals is challenging, as the process is usually governed by self organization.[129] Materials with three-dimensional structures ordered over multiple length scales can be prepared by carrying out colloidal crystallization and inorganic/organic self-assembly within microfluidic channels.[130]

Kim et al. reported the earliest result on polymeric colloidal crystallization inside PDMS channels.[131] Later on, the same group created inverted opaline structures with inorganic titania sol by infiltrating a titania precursor into the interstices of opaline structure

and subsequently removing the particles.[130] A facile route for the fabrication of cylindrical colloidal crystals (CylCCs) by self-assembly inside a microcapillary (Figure 16) was reported by Moon et al.[132] Further, inorganic inverted replicas of the CylCCs were prepared by using the shaped colloidal crystals as templates. Inorganic CylCCs were obtained by using different types of particles and microcapillaries.

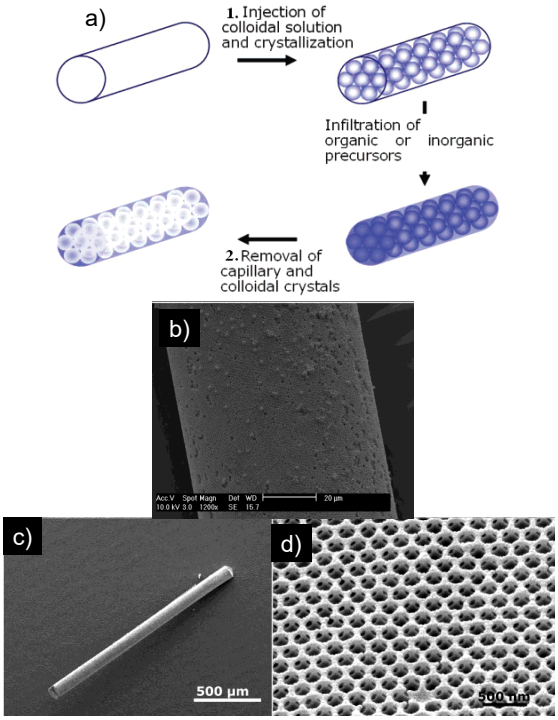

Figure 16. a) Schematic diagram for fabrication of the CylCC (1) and inverted structures from the CylCC template (2). b) SEM image of a CylCC of silica particles. The ratio of capillary to particle diameter is 65 µm/0.7 µm. c) SEM image of an ordered macroporous cylinder of silica substrate and d) surface morphology. PS beads of 0.25 µm in diameter and a PMMA capillary of 125 µm in diameter were used for the colloidal crystal template. Reproduced from ref [132], copyright American Chemical Society, 2004.

Droplets based microfluidic was also used to create self-assemblies of colloidal particles. Kim et al. encapsulated silica colloidal particles in aqueous emulsion droplets generated in oil phase by using a coflowing stream.[133] The controlled microwave irradiation of the aqueous drop led to the evaporation of the solvent and induced the self-organization of silica colloids into opaline photonic balls. Compared to conventional methods, the microwave assisted evaporation reduced the time of evaporation and the consolidation of the colloidal particles. It was also possible by controlling the microwave intensity to control the water evaporation rate. Inorganic photonic crystals with a good packing qualiy were obtained and showed photonic band gap characteristics. In-situ crystallization of colloidal particles in microfluidic chips (Figure 17) under a centrifugal force field was described in the work of Lee et al.[134] The colloidal crystallisation proceeded much faster than conventional evaporation induced crystallization. Although the processing time was dramatically reduced, the crystallinity was not seriously affected because the time scale of particles movement was still larger than the crystallization time scale. The sedimentation rate was proportional to the density difference that could be controlled by changing the dispersing media.

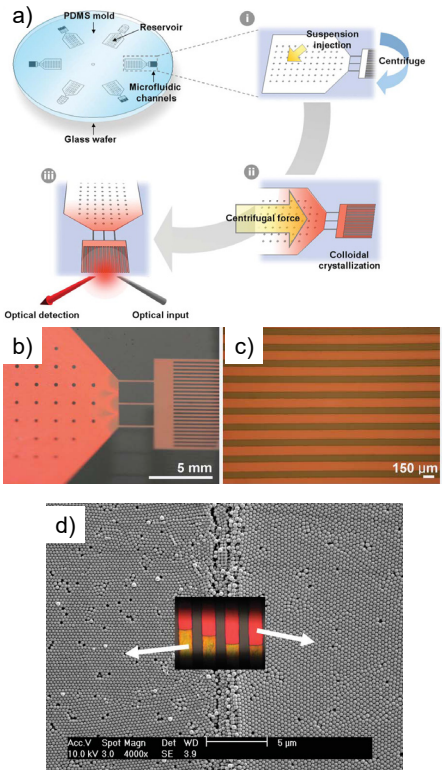

Figure 17. a) Arrangement of designed functional units of the centrifugal microfluidic chip and schematic procedure for crystallization of colloidal particles in a centrifugal microfluidic platform. Completely crystallized silica spheres of 300 nm in diameter which reflect a red colour after centrifugation: b) top view of a fluidic cell which has a set of parallel microchannels, c) colloidal crystal strips of silica spheres in microchannels. d) SEM image shows the interface of hybrid colloidal crystals composed of 255 nm and 300 nm silica particles. In the inset, the optical microscope image displays different reflection colours from two constituting parts of the hybrid colloidal crystals. Reproduced from ref [134], copyright the Royal Society of Chemistry, 2006.

4.5.2 Controlled aggregation of metal nanoparticles

The preparation at room temperature of isolated and clustered Au nanoparticles in the presence of polyelectrolyte molecules using a flow-through silicon chip reactor was reported.[111] Ascorbic acid and Fe(II) were used as reducing agents and sodium metasilicate and poly(vinyl alcohol) were added as effectors for the formation of the nanoparticles. The successive addition of reaction components in the micro-continuous flow process was tested. Single particles of different sizes, simple particles aggregates, core-shell particles as well as complex aggregates and hexagonal nanocrystallites were obtained according to the experimental conditions. Tsunoyoma and co-workers successfully prepared small PVP-stabilized gold clusters by an homogeneous mixing of continuous flows of aqueous $AuCl^4$- and BH_4^- in a micromixer (Figure 18).[135] With this method, small Au: PVP nanoparticles with a higher catalytic activity than clusters produced by conventional batch methods were prepared.

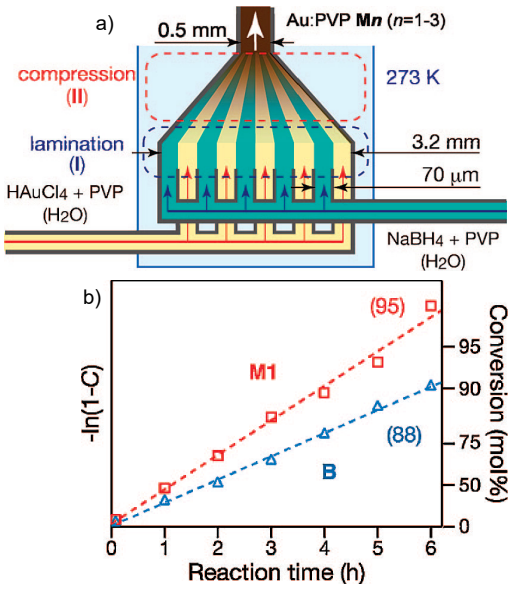

Figure 18. a) Schematic Diagram for the Synthesis of PVP-Stabilized Au Clusters in a Micromixer. b) Time course of the yield of the product p-hydroxybenzaldehyde. The numbers in parentheses indicate the isolated yields after the reactions had been conducted for 6 hours. M1 = Au:PVP prepared in microfluidic reactor. B = Au:PVP prepared by the conventional batch method. Reproduced from ref [135], copyright American Chemical Society , 2008.

4.5.3. Colloids based on inorganic materials

Chang encapsulated CdSe/ZnS QDs into uniform-sized microcapsules made of a biocompatible copolymer, poly(DL-lactide-co-glycolide) (PLGA), utilizing a microfluidic chip.[136] A blend of poly(vinyl alcohol) (PVA) and chitosan (CS) as stabilizers was formulated in order to produce the hydrophobic PLGA polymer matrix entrapping CdSe/ZnS QDs: the PLGA polymer solution was constrained to adopt the spherical droplets geometry by flowing into a continuous aqueous phase at a micro-channel T-cross junction. By adjusting the flow conditions of the two immiscible solutions, PLGA microgels encapsulating CdSe/ZnS QDs were produced with diameters ranging form 180 to 550 μm. In contrast to individual QDs, the PLGA microsphere encapsulating thousands of QDs presented a highly amplified and reproducible signal for fluorescence-based bio-analysis. In the same field of view, the encapsulation of polystyrene stabilized CdS quantum dots (PS-CdS) into mesoscale aqueous spherical assemblies named "quantum dot compound micelles" (QDCMs) was performed using either a single-phase flow-focusing reactor or a two-phase gas-segmented microfluidic reactor.[137, 138] Self-assembly was initiated by the addition of water to a blended solution of PS coated CdS nanoparticles and amphiphilic polystyrene-block-poly(acrylic acid) copolymer stabilizing chains (PS-b-PAA). In the single-phase flow focusing regime, the QDCM formation was initiated in a central stream via cross-stream diffusion of water from a surrounding sheath stream followed by a downstream quench step. In this case, on-chip size control was exerted *via* either the steady-state water concentration or the flow rate. However, QDCM polydispersities *via* this microfluidic approach were comparable to those obtained in the bulk (~30% relative standard deviations). This was partially attributed to the limitations of diffusion controlled mixing and to the large residence time distributions characteristic of single-phase reactors.

In the segmented flow approach, the QDs association was initiated by the fast mixing of the reagents via chaotic advection within liquid plugs moving through a sinusoidal channel. Subsequent recirculating flow within a post-formation channel subjected the dynamic QDCMs to shear-induced processing controlled via the flow rate and channel length before a final quench into pure water. It seemed that enhanced mixing alone was insufficient to explain the improvement in the QDCM polydispersities and that the mean sizes and the polydispersity of the assemblies immediately following association was largely governed by the steady-state water content, regardless of the very different mixing times. However, mean QDCM sizes and polydispersities were both significantly decreased in the post-formation channel by tuning the self-assembly process, which was attributed to shear-induced particle breakup within the internal back-flow fields of the liquid plugs.

Monodisperse multi-functional and mesoporous inorganic microspheres with a worm-like disordered pore structure were generated using microfluidic devices by forming uniform droplets of an aqueous-based precursor solution in a T-shaped microfluidic device followed by *ex-situ* evaporation-induced self-assembly in a batch reactor.[139] The procedure was tuned to produce well-separated particles or alternatively particles that were linked together. In order to benefit from the full potential of a microfluidic-based particle generation, Lee and co-workers described a one-step *in situ* method named "microfluidic diffusion induced self-assembly" for the synthesis of monodisperse and ordered mesoporous silica microspheres (Figure 19).[140] The method combines microfluidic generation of uniform droplets of ethanol-rich precursor phase and subsequent *in situ* rapid solvent diffusion-induced self-assembly within the microfluidic channel. Well-ordered 2D hexagonal mesostructures with an unprecedented corrugated surface morphology of disordered mesopores larger than 15 nm were prepared by this method. The surface morphology and the particle size of the mesoporous silica microspheres were systematically controlled by adjusting the microfluidic conditions.

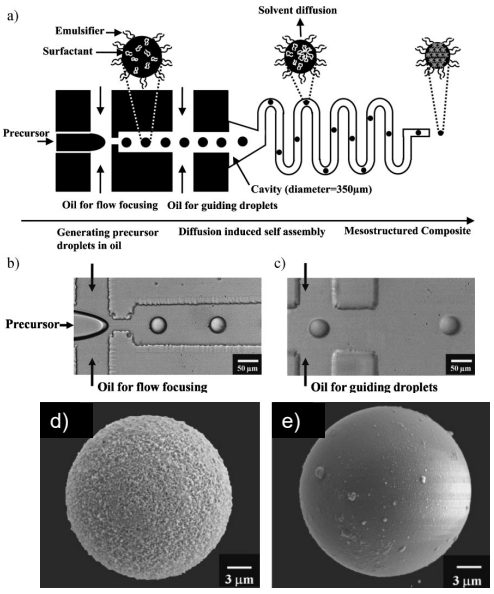

Figure 19. a) Schematic illustration of the synthesis of OMS particles using microfluidic DISA. Monodisperse droplets are generated at the T-shaped flow-focusing orifice and assembled into mesostructured silica/surfactant composite spheres via rapid diffusion-induced self-assembly (DISA) in situ within the microchannel. Optical micrographs of b) the T-shaped flow-focusing orifice generating droplets at the orifice and c) the T junction for guiding flow to prevent droplet collision by increasing interdroplet distance. Control of the surface morphology of mesoporous silica microspheres: SEM images of mesoporous silica spheres generated in d) hexadecane, e) mineral oil. Reproduced from ref [140], copyright Wiley-VCH Verlag GmbH & Co. KGaA., 2008..

In situ preparation of monodisperse hybrid Janus microspheres (HJM) with inorganic allylhydridopolycarbosilane and organic perfluoropolyether parts was demonstrated by using a hydrodynamic flow-focusing device.[141] A photocurable oligomer solution was generated into an immiscible continuous phase. The size and shape of the HJM was controlled by varying the flow rate of the oligomer solution and of the continuous phase. The selective incorporation of magnetic Fe_3O_4 into the inorganic allylhydridopolycarbosilane lobe of the HJM was performed in order to produce microspheres displaying a magnetic field induced behaviour.

Single-step fabrication of TiO_2 microspheres with embedded functional CdS and Fe_2O_3 nanoparticles were also fabricated in a three dimensional co-flows microfluidic device.[142] The functional nanoparticles were confined mainly in the titania shells of the resulting hollow spheres, which were highly monodisperse and with a good stability against coagulation.

5. Conclusions and outlook

This review aimed to cover different aspects of microfluidics in the field of inorganic chemistry. The high area/volume ratio and the significantly reduced diffusion distance in microfluidic systems are the most commonly known advantages appealing the chemists to adapt their chemical applications of interest at a microfluidic scale. In the field of inorganic extraction, innovative works have been done but were limited to the simple separation of a few metallic species. The microfluidic synthesis of inorganic or bioinorganic molecular compounds or clusters in their discrete or crystalline forms also remains poorly explored. In the field of inorganic chemistry, microfluidic processes until now have mainly focused on the optimization of nanomaterials synthesis. Compared to conventional methods, the physical properties were improved and a better control of the size and the polydispersity of particles were possible. A great interest was brought to quantum dots. This is probably due to the easiness to use on-line characterization methods (absorption and fluorescence spectroscopy) to study their synthesis process. Fluorescence has been mostly used because of its simplicity of implementation in microscopic formats and its widespread use as a sensitive and quantitative spectroscopic tool. Nevertheless, most inorganic materials are not fluorescent, and characterization has to be completed by using off-line analytical methods as X-ray spectroscopy or Transmission Electron Microscopy. On-line integration of analysis within the microchemical systems would allow a better optimization and access to the kinetic parameters of the chemical reactions. Integration and development of analytical methods as electrophoresis,[66] NMR,[143-145] mass spectroscopy,[146] FTIR,[147] IR,[148] Raman[149-151] devoted for kinetic studies of organic reactions have been described. However in the field of inorganic materials chemistry UV-Vis spectroscopy seems to be the only- in situ- available method. Very recently, a free jet micromixer was coupled to small angle X-ray scattering (SAXS) on a synchrotron beamline to acquire kinetic data on the nucleation and growth of nanoparticles.[152] It is a very powerful technique but it cannot be coupled so easily to microfluidic devices. This difficulty to find a convenient technique to ensure an on-line characterization of nanoparticles is an important limitation to achieve the optimization of inorganic synthesis in microreactors and development of on line characterization methods has to be the priority in the next few years.

Addendum (January 29, 2010)

Performing inorganic chemical reactions in microchannels has been increasingly established as a method for the preparation of inorganic nanomaterials. During the time since submission of this Review, new papers have been published in the field of inorganic chemistry using microfluidics. These publications cover new techniques and devices for the comprehension of fundamental aspects of this chemistry as nucleation and growth of nanoparticles,[153] the synthesis of metallic nanoparticles with different shapes,[154] quantum dots and oxide nanoparticles.[155-158]

Received: July 31, 2009
Accepted: February 1, 2010
Published online: August 2, 2010

[1] A. Manz, N. Graber, H. M. Widmer, *Sensors and Actuators B: Chemical* **1990**, *1*, 244-248.
[2] A. Manz, D. J. Harrison, E. Verpoorte, J. C. Fettinger, H. Lundi, M. Widmer, *Chimia* **1991**, *45*, 103-105.
[3] A. Manz, D. J. Harrison, E. Verpoorte, M. Widmer, *Adv. Chromatogr.* **1993**, *33*, 1.
[4] A. Van den Berg, T. S. J. Lammerink, *Top. Curr. Chem.* **1998**, *194*, 21.
[5] P. S. Dittrich, A. Manz, *Nat Rev Drug Discov* **2006**, *5*, 210-218.
[6] J. M. Ramsey, S. C. Jacobson, M. R. Knapp, *Nat Med* **1995**, *1*, 1093-1095.
[7] S. J. Haswell, P. Watts, *Green Chemistry* **2003**, *5*, 240-249.
[8] J.-i. Yoshida, A. Nagaki, T. Yamada, *Chem. Eur. J.* **2008**, *14*, 7450-7459.
[9] B. Detlev, *Angew. Chem. Int. Ed.* **2009**, *48*, 3736-3737.
[10] a) W. Ehrfeld, V. Hessel, H. Löwe, Microreactors: New Technology for Modern Chemistry, Wiley VCH, Weinheim, **2000**; b) V. Hessel, H. Löwe, A. Müller, G. Kolb, Chemical Micro Process Engineering. Fundamentals, Modelling and Reactions/Processes and Plants, Wiley-VCH, Weinheim, **2005**; c) N. Kockmann, O. Brand, G. K. Fedder, Micro Process Engineering, Wiley-VCH, Weinheim **2006**; d) J. Yoshida, Flash Chemistry. Fast Organic Synthesis in Microsystems, Wiley-Blackwell, **2008**; e) V. Hessel, J. C. Schouten, A. Renken, J. Yoshida Eds. Micro Process Engineering, A Comprehensive Handbook, Wiley, **2009**.
[11] G. M. Whitesides, *Nature* **2006**, *442*, 368-373.
[12] J. West, M. Becker, S. Tombrink, A. Manz, *Anal. Chem.* **2008**, *80*, 4403-4419.
[13] D. Psaltis, S. R. Quake, C. Yang, *Nature* **2006**, *442*, 368-373.
[14] A. J. deMello, *Nature* **2006**, *442*, 394-402.
[15] M. Joanicot, A. Ajdari, *Science* **2005**, *309*, 887-888.
[16] D. M. Ratner, E. R. Murphy, M. Jhunjhunwala, D. A. Snyder, K. F. Jensen, P. H. Seeberger, *Chem. Commun.* **2005**, 578-580.
[17] R. D. Chambers, M. A. Fox, D. Holling, T. Nakano, T. Okazoe, G. Sandford, *Lab Chip* **2005**, *5*, 191-198.
[18] J. Knight, *Nature* **2002**, *418*, 474-475.
[19] J. Hogan, *Nature* **2006**, *442*, 351-352.
[20] H. A. Stone, A. D. Stroock, A. Ajdari, *Annu. Rev. Fluid Mech.* **2004**, *36*, 381-411.
[21] T. M. Squires, S. R. Quake, *Rev.Mod. Phys.* **2005**, *77*, 977-1026.
[22] K. Jähnisch, V. Hessel, H. Löwe, M. Baerns, Angew. Chem. **2004**, *116*, 410-451; *Angew. Chem. Int. Ed.* **2004**, *43*, 406-446.
[23] J. Kobayashi, Y. Mori, K. Okamoto, R. Akiyama, M. Ueno, T. Kitamori, S. Kobayashi, *Science* **2004**, *304*, 1305-1308.
[24] C. L. Hansen, E. Skordalakes, J. M. Berger, S. R. Quake, *Proc. Natl. Acad. Sci. USA* **2002**, *99*, 16531-16536.
[25] J. Atencia, D. J. Beebe, *Nature* **2005**, *437*, 648-655.
[26] N.-T. Nguyen, Z. Wu, *J. Micromech. Microeng.* **2005**, R1-R16.
[27] J. M. Ottino, S. Wiggins, *Phil. Trans. R. Soc. Lond. A* **2004**, *362*, 923 - 935.
[28] H. Lowe, W. Ehrfeld, *Electrochim. Acta.* **1999**, *44*, 3679–3689
[29] P. Tabeling, *Introduction to microfluidics*, Oxford University Press ed., **2005**.
[30] J. B. Knight, A. Vishwanath, J. P. Brody, R. H. Austin, *Phys. Rev. Lett.* **1998**, *80*, 3863 - 3866.

[31] H. Song, D. L. Chen, R. F. Ismagilov Angew. Chem. **2003**, *115*, 792-796; Angew. Chem. Int. Ed. **2003**, *42*, 768-772

[32] B. K. H. Yen, A. Günther, M. A. Schmidt, K. F. Jensen, M. G. Bawendi, Angew. Chem. **2005**, *117*, 5583-5587 Angew. Chem. Int. Ed. **2005**, *44*, 5447-5451.

[33] E. A. Mansur, M. Ye, Y. Wang, Y. Dai, *Chin. J. Chem. Eng.* **2008**, *16*, 503-516.

[34] A. Günther, K. F. Jensen, *Lab. Chip* **2006**, *6*, 1487 - 1503,.

[35] J. M. Ottino, *Ann. Rev. Fluid Mech.* **1990**, *22*, 207-254.

[36] V. Hessel, H. Löwe, F. Schönfeld, *Chem. Eng. Sci.* **2005**, *60*, 2479-2501.

[37] W. Ehrfeld, V. Hessel, H. Lowe, *Microreactors*, Wiley-VCH, Weinheim, **2000**.

[38] P. Gravesen, J. Branjeberg, O. S. Jensen, in *Micro Mechanics Europe, MME'93*, Neuchatel, Switzerland, **1993**, p. 143.

[39] K. F. Jensen, *Chem. Eng. Sci.* **2001**, *56*, 293-303.

[40] C. Alépée, L. Vulpescu, P. Cousseau, P. Renaud, R. Maurer, A. Renken, in *IMRET 4 : 4th International Conference on Microreaction Technology*, American Institute of Chemical Engineers Topical Conference Proceedings, Atlanta, USA, **2000**, p. 71.

[41] H. Pennemann, V. Hessel, H. Löwe, *Chem. Eng. Sci.* **2004**, *59*, 4789-4794.

[42] G. N. Doku, W. Verboom, D. N. Reinhoudt, A. van den Berg, *Tetrahedron* **2005**, *61*, 2733-2742.

[43] H. R. Sahoo, J. G. Kralj, K. F. Jensen, *Angew. Chem. Int. Ed.* **2007**, *46*, 5704-5708.

[44] A. Abou-Hassan, O. Sandre, S. Neveu, V. Cabuil *Angew. Chem.* **2009**, *121*, 2378-2381; *Angew. Chem. Int. Ed.* **2009**, *48*, 2342-2345.

[45] M. Tokeshi, T. Minagawa, K. Uchiyama, A. Hibara, K. Sato, H. Hisamoto, T. Kitamori, *Anal. Chem.* **2002**, *74*, 1565-1571.

[46] B. K. H. Yen, N. E. Stott, K. F. Jensen, M. G. Bawendi, *Adv. Mater.* **2003**, *15*, 1858-1862.

[47] H. Song, D. L. Chen, R. F. Ismagilov Angew. Chem. **2006**, *118*, 7494-7516; Angew. Chem. Int. Ed. **2006**, *45*, 7336-7356

[48] H. Hotokezaka, M. Tokeshi, M. Harada, T. Kitamori, Y. Ikeda, *Progress in Nuclear Energy* **2005**, *47*, 439-447.

[49] M. Tokeshi, T. Kitamori, *Progress in Nuclear Energy* **2005**, *47*, 434-438.

[50] K. Sato, M. Tokeshi, T. Sawada, T. Kitamori, *Anal. Sci.* **2000**, *16*, 455-456.

[51] M. Tokeshi, M. Uchida, A. Hibara, T. Sawada, T. Kitamori, *Anal. Chem.* **2001**, *73*, 2112-2116.

[52] H.-B. Kim, K. Ueno, M. Chiba, O. Kogi, N. Kitamura, *Anal. Sci.* **2000**, *16*, 871-876.

[53] M. Tokeshi, T. Minagawa, T. Kitamori, *Anal. Chem.* **2000**, *72*, 1711-1714.

[54] T. Minagawa, M. Tokeshi, T. Kitamori, *Lab Chip* **2001**, *1*, 72-75.

[55] M. Tokeshi, T. Minagawa, T. Kitamori, *J. Chromatogr. A* **2000**, *894*, 19-23.

[56] T. Maruyama, T. Kaji, T. Ohkawa, K.-i. Sotowa, H. Matsushita, F. Kubota, N. Kamiya, K. Kusakabe, M. Goto, *Analyst* **2004**, *129*, 1008-1013.

[57] A. Hibara, M. Tokeshi, K. Uchiyama, H. Hisamoto, T. Kitamori, *Anal. Sci.* **2001**, *17*, 89-93.

[58] T. Maruyama, H. Matsushita, J.-i. Uchida, F. Kubota, N. Kamiya, M. Goto, *Anal. Chem.* **2004**, *76*, 4495-4500.

[59] H. Hisamoto, T. Horiuchi, K. Uchiyama, M. Tokeshi, A. Hibara, T. Kitamori, *Anal. Chem.* **2001**, *73*, 5551-5556.

[60] M. Kumemura, T. Korenaga, *Analytica Chimica Acta* **2006**, *558*, 75-79.

[61] H. Shen, Q. Fang, Z.-L. Fang, *Lab Chip* **2008**, *6*, 1387 - 1389.

[62] D. Kashciev, *Nucleation Basic Theory with Applications*, Butterworth-Heinemann, **2000**.

[63] K. F. Jensen, *MRS Bull.* **2006**, *31*, 101-107.

[64] Y. Song, J. Hormes, C. S. S. R. Kumar, *Small* **2008**, *4*, 698-711.

[65] Y. Xia, G. M. Whitesides, *Ann. Rev. Mater. Sci.* **1998**, *28*, 153-184.

[66] B. Detlev, L. Martin, W. Li-Wen, T. R. Manfred Angew. Chem. **2006**, *118*, 2373-2376; Angew. Chem. Int. Ed., **2006**, *45*, 2463-2466

[67] A. J. deMello, J. C. deMello, *Lab Chip* **2004**, *4*, 11N-15N.

[68] L.-H. Hung, A. P. Lee, *J. Med. Biol. Eng.* **2007**, *27*, 1-6.

[69] G. I. Taylor, *Proc. R. Soc. London. Ser. A* **1953**, *219*, 186-203.

[70] P. Laval, A. Crombez, J.-B. Salmon, *Langmuir* **2009**, *25*, 1836-1841.

[71] J. B. Edel, R. Fortt, J. C. deMello, A. J. deMello, *Chem. Commun.* **2002**, 1136-1137.

[72] A. P. Alivisatos, *Science* **1996**, *271*, 933-937.

[73] M. A. Hines, P. Guyot-Sionnest, *J. Phys. Chem.* **1996**, *100*, 468-471.

[74] C. B. Murray, C. R. Kagan, M. G. Bawendi, *Annu. Rev. Mater. Sci.* **2000**, *30*, 545-610.

[75] C. D. Dushkin, S. Saita, K. Yoshie, Y. Yamaguchi, *Adv. Colloid Interf. Sci.* **2000**, *88*, 37-78.

[76] E. M. Chan, R. A. Mathies, A. P. Alivisatos, *Nano. Lett.* **2003**, *3*, 199-201.

[77] F. G. Bessoth, A. J. deMello, A. Manz, *Anal. Commun.* **1999**, *36*, 213 - 215.

[78] I. Shestopalov, J. D. Tice, R. F. Ismagilov, *Lab Chip* **2004**, *4*, 316-321.

[79] L.-H. Hung, K. M. Choi, W.-Y. Tseng, Y.-C. Tan, K. J. Shea, A. P. Lee, *Lab Chip* **2006**, *6*, 174-178.

[80] T. L. Sounart, P. A. Safier, J. A. Voigt, J. Hoyt, D. R. Tallant, C. M. Matzke, T. A. Michalske, *Lab. Chip* **2007**, *7*, 908-915.

[81] H. Nakamura, Y. Yamaguchi, M. Miyazaki, H. Maeda, M. Uehara, P. Mulvaney, *Chem. Commun.* **2002**, 2844-2845.

[82] S. Krishnadasan, J. Tovilla, R. Vilar, A. J. deMello, J. C. deMello, *J. Mater.Chem.* **2004**, *14*, 2655-2660.

[83] E. M. Chan, A. P. Alivisatos, R. A. Mathies, *J. Am. Chem. Soc.* **2005**, *127*, 13854-13861.

[84] S. Marre, J. Park, J. Rempel, J. Guan, M. G. Bawendi, K. F. Jensen, *Adv. Mater.* **2008**, *20*, 4830-4834.

[85] H. Yang, W. Luan, S.-t. Tu, Z. M. Wang, *Lab. Chip* **2008**, *8*, 451 - 455.

[86] A. Singh, M. Limaye, S. Singh, L. Niranjan Prasad, C. K. Malek, S. Kulkarni, *Nanotechnology* **2008**, 245613.

[87] A. Abou-Hassan, R. Bazzi, V. Cabuil Angew. Chem. **2009**, *121*, 7316-7319; Angew. Chem. Int. Ed. **2009**, *48*, 7180-7183

[88] M. Bruchez, Jr., M. Moronne, P. Gin, S. Weiss, A. P. Alivisatos, *Science* **1998**, *281*, 2013-2016.

[89] B. O. Dabbousi, J. Rodriguez-Viejo, F. V. Mikulec, J. R. Heine, H. Mattoussi, R. Ober, K. F. Jensen, M. G. Bawendi, *J. Phys. Chem. B* **1997**, *101*, 9463-9475.

[90] H. Wang, X. Li, M. Uehara, Y. Yamaguchi, H. Nakamura, M. Miyazaki, H. Shimizu, H. Maeda, *Chem. Commun.* **2004**, 48-49.

[91] H. Wang, H. Nakamura, M. Uehara, Y. Yamaguchi, M. Miyazaki, H. Maeda, *Adv. Funct. Mater.* **2005**, *15*, 603-608.

[92] W. Luan, H. Yang, N. Fan, S.-T. Tu, *Nanoscale Res. Lett.* **2008**, *3*, 134-139.

[93] M. Uehara, H. Nakamura, H. Maeda, in *World Congress on Medical Physics and Biomedical Engineering 2006*, **2007**, pp. 250-253.

[94] H. Wang, H. Nakamura, M. Uehara, M. Miyazaki, H. Maeda, *Chem. Commun.* **2002**, 1462-1463.

[95] M. Takagi, T. Maki, M. Miyahara, K. Mae, *Chem. Eng. J.* **2004**, *101*, 269-276.

[96] B. F. Cottam, S. Krishnadasan, A. J. DeMello, J. C. DeMello, M. S. P. Shaffer, *Lab Chip* **2007**, *7*, 167-169.

[97] H. Nagasawa, T. Tsujiuchi, T. Maki, K. Mae, *AIChE Journal* **2007**, *53*, 196-206.

[98] S. A. Khan, A. Gunther, M. A. Schmidt, K. F. Jensen, *Langmuir* **2004**, *20*, 8604-8611.

[99] A. Abou Hassan, O. Sandre, V. Cabuil, P. Tabeling, *Chem. Commun.* **2008**, 1783-1785.

[100] L. Frenz, A. El Harrak, M. Pauly, S. Bégin-Colin, Andrew D. Griffiths, J.-C. Baret Angew. Chem. **2008**, *120*, 6923-6926; Angew. Chem. Int. Ed. **2008**, *47*, 6817-6820

[101] T. Miyake, T. Ueda, N. Ikenaga, H. Oda, M. Sano, *J. Mater. Sci.* **2005**, *40*, 5011-5013.

[102] W. Stober, A. Fink, A. Bohn, *J. Colloid. Interface. Sci.* **1968**, *26*, 62-69.

[103] R. Massart, *IEEE Trans. Magn.* **1981**, *17*, 1247-1250.

[104] S. A. Khan, K. F. Jensen, *Adv. Mater.* **2007**, *19*, 2556-2560.

[105] F. Kim, J. H. Song, P. Yang, *J. Am. Chem. Soc* **2002**, *124*, 14316-14317.

[106] K. Akamatsu, S. Deki, *J. Mater. Chem.* **1997**, *7*, 1773 - 1777.

[107] M. Kogiso, K. Yoshida, K. Yase, T. Shimizu, *Chem. Commun.* **2002**, 2492 - 2493.

[108] J. A. Eastman, S. U. S. Choi, S. Li, W. Yu, L. J. Thompson, *Appl. Phys. Lett.* **2001**, *78*, 718-720.

[109] J. Wagner, T. Kirner, G. Mayer, J. Albert, J. M. Köhler, *Chem. Eng. Sci.* **2004**, *101*, 251-260.

[110] J. Wagner, J. M. Kohler, *Nano Lett.* **2005**, *5*, 685-691.

[111] J. M. Kohler, J. Wagner, J. Albert, *J. Mater. Chem.* **2005**, *15*, 1924-1930.
[112] J. Boleininger, A. Kurz, V. Reuss, C. Sonnichsen, *Phys. Chem. Chem. Phys.* **2006**, *8*, 3824-3827.
[113] J. Wagner, T. R. Tshikhudo, J. M. Köhler, *Chem. Eng. J.* **2008**, *135*, S104-S109.
[114] J. M. Köhler, L. Abahmane, J. Wagner, J. Albert, G. Mayer, *Chem. Eng. Sci.* **2008**, *63*, 5048-5055.
[115] X. Z. Lin, A. D. Terepka, H. Yang, *Nano Lett.* **2004**, *4*, 2227-2232.
[116] Y. Song, E. E. Doomes, J. Prindle, R. Tittsworth, J. Hormes, C. S. S. R. Kumar, *J. Phys. Chem. B.* **2005**, *109*, 9330-9338.
[117] Y. Song, C. S. S. R. Kumar, J. Hormes, *J. Nanosci. Nanotech.* **2004**, *4*, 788-793.
[118] P. Mulvaney, *Langmuir* **1996**, *12*, 788-800.
[119] N. R. Jana, L. Gearheart, C. J. Murphy, *Adv. Mater.* **2001**, *13*, 1389-1393.
[120] M.-L. Wu, D.-H. Chen, T.-C. Huang, *Chem. Mater.* **2001**, *13*, 599-606.
[121] B. Nikoobakht, M. A. El-Sayed, *Chem. Mater.* **2003**, *15*, 1957-1962.
[122] C. Wu, T. Zeng, *Chem. Mater.* **2007**, *19*, 123-125.
[123] H. Nagasawa, K. Mae, *Ind. Eng. Chem. Res.* **2006**, *45*, 2179-2186.
[124] S. Zinoveva, R. De Silva, R. D. Louis, P. Datta, C. S.S.R. Kumar, J. Goettert, J. Hormes, *Nucl. Instrum. Methods Phys. Res. Sect. A* **2007**, *582*, 239-241.
[125] A. van Blaaderen, R. Ruel, P. Wiltzius, *Nature* **1997**, *385*, 321-324.
[126] J.-Y. Shiu, C.-W. Kuo, P. Chen, *J. Am. Chem. Soc* **2004**, *126*, 8096-8097.
[127] G.-R. Yi, S.-J. Jeon, T. Thorsen, V. N. Manoharan, S. R. Quake, D. J. Pine, S.-M. Yang, *Synthetic Metals* **2003**, *139*, 803-806.
[128] J. H. Moon, G. R. Yi, S. M. Yang, D. J. Pine, S. B. Park, *Adv. Mater.* **2004**, *16*, 605-609.
[129] S.-K. Lee, S.-H. Kim, J.-H. Kang, S.-G. Park, W.-J. Jung, S.-H. Kim, G.-R. Yi, S.-M. Yang, *Microfluid. Nanofluid.* **2008**, *4*, 129-144.
[130] P. Yang, A. H. Rizvi, B. Messer, B. F. Chmelka, G. M. Whitesides, G. D. Stucky, *Adv. Mater.* **2001**, *13*, 427-431.
[131] E. Kim, Y. Xia, G. M. Whitesides, *Adv. Mater.* **1996**, *8*, 245-247.
[132] J. H. Moon, S. Kim, G.-R. Yi, Y.-H. Lee, S.-M. Yang, *Langmuir* **2004**, *20*, 2033-2035.
[133] S.-H. Kim, S. Y. Lee, G.-R. Yi, D. J. Pine, S.-M. Yang, *J. Am. Chem. Soc* **2006**, *128*, 10897-10904.
[134] S.-K. Lee, G.-R. Yi, S.-M. Yang, *Lab Chip* **2006**, *6*, 1171-1177.
[135] H. Tsunoyama, N. Ichikuni, T. Tsukuda, *Langmuir* **2008**, *24*, 11327-11330.
[136] J.-Y. Chang, C.-H. Yang, K.-S. Huang, *Nanotechnology* **2007**, 305305.
[137] G. Schabas, H. Yusuf, M. G. Moffitt, D. Sinton, *Langmuir* **2008**, *24*, 637-643.
[138] G. Schabas, C.-W. Wang, A. Oskooei, H. Yusuf, M. G. Moffitt, D. Sinton, *Langmuir* **2008**, *24*, 10596-10603.
[139] N. J. Carroll, S. B. Rathod, E. Derbins, S. Mendez, D. A. Weitz, D. N. Petsev, *Langmuir* **2008**, *24*, 658-661.
[140] I. Lee, Y. Yoo, Z. Cheng, H.-K. Jeong, *Adv. Funct. Mat.* **2008**, *18*, 4014-4021.
[141] N. Prasad, J. Perumal, C.-H. Choi, C.-S. Lee, D.-P. Kim, *Adv. Funct. Mater.* **2009**, *19*, 1656-1662.
[142] T. H. Eun, S.-H. Kim, W.-J. Jeong, S.-J. Jeon, S.-H. Kim, S.-M. Yang, *Chem. Mater.* **2009**, *21*, 201-203.
[143] H. Wensink, F. Benito-Lopez, D. C. Hermes, W. Verboom, H. J. G. E. Gardeniers, D. N. Reinhoudt, A. v. d. Berg, *Lab Chip* **2005**, *5*, 280-284.
[144] J. Bart, A. J. Kolkman, A. J. Oosthoek-de Vries, K. Koch, P. J. Nieuwland, H. Janssen, J. van Bentum, K. A. M. Ampt, F. P. J. T. Rutjes, S. S. Wijmenga, H. Gardeniers, A. P. M. Kentgens, *J. Am. Chem. Soc.* **2009**, *131*, 5014-5015.
[145] L.-S. Bouchard, S. R. Burt, M. S. Anwar, K. V. Kovtunov, I. V. Koptyug, A. Pines, *Science* **2008**, *319*, 442-445.
[146] L. M. Fidalgo, G. Whyte, B. T. Ruotolo, J. L. P. Benesch, F. Stengel, C. Abell, C. V. Robinson, W. T. S. Huck Angew. Chem. **2009**, *121*, 3719-3722; Angew. Chem. Int. Ed. **2009**, *48*, 3665-3668.
[147] R. Herzig-Marx, K. T. Queeney, R. J. Jackman, M. A. Schmidt, K. F. Jensen, *Anal. Chem.* **2004**, *76*, 6476-6483.
[148] T. M. Floyd, M. A. Schmidt, K. F. Jensen, *Ind. Eng. Chem. Res.* **2004**, *44*, 2351-2358.
[149] S.-A. Leung, R. F. Winkle, R. C. R. Wootton, A. J. deMello, *Analyst* **2005**, *130*, 46-51.
[150] D. Schafer, J. A. Squier, J. v. Maarseveen, D. Bonn, M. Bonn, M. Muller, *J. Am. Chem. Soc.* **2008**, *130*, 11592-11593.
[151] F. Sarrazin, J.-B. Salmon, D. Talaga, L. Servant, *Anal. Chem.* **2008**, *80*, 1689-1695.
[152] B. Marmiroli, G. Grenci, F. Cacho-Nerin, B. Sartori, E. Ferrari, P. Laggner, L. Businaro, H. Amenitsch, *Lab Chip* **2009**, *9*, 2063-2069.
[153] J. R. Polte, R. Erler, A. F. Thunemann, S. Sokolov, T. T. Ahner, K. Rademann, F. Emmerling, R. Kraehnert, *ACS Nano* **2010**; DOI: 10.1021/nn901499c.
[154] D. Suhanya, A. K. Saif, *Small* **2009**, 5, 2828-2834.
[155] M. N. Adrian, C. d. M. John, *ChemPhysChem* **2009**, 10, 2612-2614.
[156] W.-B. Lee, C.-H. Weng, F.-Y. Cheng, C.-S. Yeh, H.-Y. Lei, G.-B. Lee, *Biomed. Microdev.* **2009**, 11, 161-171.
[157] K. Shiba, M. Ogawa, *Chem. Comm*. **2009**, 6851-6853.
[158] J. Wacker, V. K. Parashar, M. A. M. Gijs, *Procedia Chemistry* **2009**, 1, 377-380.

Author manuscript version of Angewandte Chemie International Edition, 2010. **49**(36): 6268-6286

Entry for the Table of Contents

Layout 1:

Inorganic in microfluidics

Ali Abou-Hassan*, Olivier Sandre and Valérie Cabuil*_____

Page1 – Page19

((Microfluidics in Inorganic Chemistry))

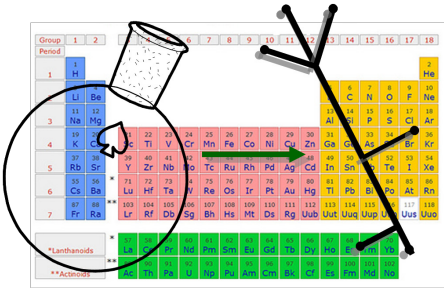

Microreactors have been proposed as a new and convenient tool for the liquid-liquid extraction and the optimization of chemical inorganic reactions. Fundamental studies in the field of inorganic chemistry have been carried out thanks to microfluidics, to understand the phenomena of nucleation and growth during the chemical process. This Review provides up-to-date data and discusses the role of microfluidics in the field of inorganic chemistry.